

# Multimodal large language model for wheat breeding: a new exploration of smart breeding

Guofeng Yang<sup>a</sup>, Yu Li<sup>b</sup>, Yong He<sup>a</sup>, Zhenjiang Zhou<sup>a</sup>, Lingzhen Ye<sup>c</sup>, Hui Fang<sup>a</sup>, Yiqi Luo<sup>d</sup>, Xuping Feng<sup>a\*</sup>

## Affiliations

<sup>a</sup> *College of Biosystems Engineering and Food Science, Zhejiang University, Hangzhou 310058, Zhejiang, China*

<sup>b</sup> *Zhejiang Society of Agricultural Machinery, Hangzhou 310003, Zhejiang, China*

<sup>c</sup> *College of Agriculture and Biotechnology, Zhejiang University, Hangzhou 310058, Zhejiang, China*

<sup>d</sup> *Soil and Crop Sciences Section, School of Integrative Plant Science, Cornell University, Ithaca 14853, New York, USA*

\*Correspondence: fengxp@zju.edu.cn

## Abstract

UAV remote sensing technology has become a key technology in crop breeding, which can achieve high-throughput and non-destructive collection of crop phenotyping data. However, the multidisciplinary nature of breeding has brought technical barriers and efficiency challenges to knowledge mining. Therefore, it is important to develop a smart breeding goal tool to mine cross-domain multimodal data. Based on different pre-trained open-source multimodal large language models (MLLMs) (e.g., Qwen-VL, InternVL, Deepseek-VL), this study used supervised fine-tuning (SFT), retrieval-augmented generation (RAG), and reinforcement learning from human feedback (RLHF) technologies to inject cross-domain knowledge into MLLMs, thereby constructing multiple multimodal large language models for wheat breeding (WBLMs). The above WBLMs were evaluated using the newly created evaluation benchmark in this study. The results showed that the WBLM constructed using SFT, RAG and RLHF technologies and InternVL2-8B has leading performance. Then, subsequent experiments were conducted using the WBLM. Ablation experiments indicated that the

combination of SFT, RAG, and RLHF technologies can improve the overall generation performance, enhance the generated quality, balance the timeliness and adaptability of the generated answer, and reduce hallucinations and biases. The WBLM performed best in wheat yield prediction using cross-domain data (remote sensing, phenotyping, weather, germplasm) simultaneously, with  $R^2$  and RMSE of 0.821 and 489.254 kg/ha, respectively. Furthermore, the WBLM can generate professional decision support answers for phenotyping estimation, environmental stress assessment, target germplasm screening, cultivation technique recommendation, and seed price query tasks. This study aims to provide intelligent and integrated solutions for wheat breeding goals, to help breeding work be carried out efficiently, to accelerate the breeding process of excellent varieties, and to provide scientific basis and technical support for achieving sustainable agricultural development and ensuring food security.

### **Keywords**

Data fusion; Remote sensing; Multimodal large language model; Cross-domain knowledge; Smart breeding

### **1. Introduction**

As one of the basic food crops for mankind, wheat breeding is facing unprecedented challenges and opportunities due to the global food crisis and the promotion of sustainable agricultural development (Cheng et al., 2024; Senapati et al., 2022). Although traditional breeding methods have achieved remarkable results, their efficiency and accuracy have gradually revealed their limitations in the face of complex and changing climatic conditions, increasingly serious threats from pests and diseases, and constantly upgrading consumer demands (Hu et al., 2022; Xiong et al., 2021). Due to the diversity of wheat varieties, breeding information has long lacked a unified tool, and data knowledge has shown an "isolated" distribution, which has created barriers to the learning of wheat breeding knowledge (Bhat et al., 2023). Simultaneously, since wheat breeding involves the intersection of multiple disciplines such as biology, genetics, weather, and soil science, professionals have to cross literature and data from

many fields when engaged in breeding work, and even need to write code to access data, which greatly limits their work efficiency (Kaur et al., 2021). Smart breeding, as an innovative mode that integrates modern information technology, biotechnology, and agricultural science, is gradually becoming a key path to solving this problem (H. Li et al., 2024; Xu et al., 2022).

With the rapid development of unmanned aerial vehicle (UAV) technology, its application in the agricultural field has become more and more extensive, especially UAVs have shown great potential in intelligent breeding (Das et al., 2021; Fei et al., 2023; Jiang et al., 2021). With its advantages of high efficiency, precision and flexibility, it is becoming an indispensable tool in smart breeding and can provide important monitoring data for smart breeding. Image recognition technology can accurately extract wheat growth indicators from RS images, such as chlorophyll content (Feng et al., 2023; Zhang et al., 2024) and leaf area index (Chen et al., 2022; Du et al., 2023); text analysis technology can extract valuable germplasm descriptions (L. Liu et al., 2024; Sansaloni et al., 2020), breeding optimization strategies (J. Xu et al., 2023; Yao et al., 2022) and market trends (Garg et al., 2022; Padhy et al., 2024) from research manuscripts, reports and databases. The complementarity of image and text information not only enhances the credibility and interpretability of the data, but also promotes the integration of interdisciplinary knowledge, opening up new avenues for wheat breeding research. At present, there is an urgent need to integrate cross-domain data (RS data, phenotyping data, environment data, germplasm data, cultivation data, and price data), use artificial intelligence algorithms and big data technology to build a cross-scale and cross-domain comprehensive analysis tool for wheat breeding, accelerate the screening and optimization of wheat target varieties, and improve the efficiency and accuracy of wheat breeding.

In recent years, the large language model (LLM) has attracted much attention due to their powerful text generation and understanding capabilities (X. Huang et al., 2024; Lin et al., 2024). After fine-tuning, the LLM has shown strong interactive capabilities and the potential to improve productivity (Min et al., 2024). However, since the LLM can only process plain text and cannot process images, voice, and video, their

application scope is limited (Wang et al., 2023). In the context of cross-domain, multi-modal data fusion applications, several multimodal large language models (MLLM) have been developed to enhance the ability of LLM to perceive and understand visual signals (AI et al., 2024, p. 0; Bai et al., 2023; Z. Chen et al., 2024; DeepSeek-AI et al., 2024; GLM et al., 2024; F. Li et al., 2024). Although a lot of study has been done to explore the limitations and effectiveness of MLLM, the current open-source general MLLM still has the problem of insufficient accuracy in professional applications (D. Huang et al., 2024; C. Li et al., 2024), such as wheat breeding selection. When faced with wheat breeding query, general MLLM often evades the question or gives irrelevant answers due to lack of breeding knowledge. This hinders the further exploration and application of MLLM in the field of wheat breeding.

However, the research and application of MLLM in crop breeding is still in its early stages and faces many challenges and opportunities (Zhu et al., 2024). The MLLM needs to integrate more complex data from different sources, including but not limited to RS data, phenotyping data, and environment data during the crop growth period. Data from these sources vary significantly in format, dimensionality, and sparsity. How to efficiently and accurately integrate these cross-domain heterogeneous data is a difficulty in current research (Kuska et al., 2024). MLLM needs to have strong learning and generalization capabilities to adapt to the needs of smart breeding and predict the performance of crops under different environmental conditions, which places extremely high demands on the model's algorithm design and computing resources. Additionally, professional knowledge and experience in the field of crop breeding are crucial for the development and application of the model (J. Li et al., 2024). How to integrate professional knowledge into model design to make the model more in line with actual breeding needs, while discovering new breeding strategies and optimization solutions through the model, is another issue that needs in-depth exploration. MLLM is expected to reveal the deep mechanisms of crop trait formation by integrating cross-modal information and accelerate the screening and breeding process of new varieties.

This study aims to innovatively construct a MLLM for wheat breeding (WBLM) through cross-domain data fusion and cutting-edge technology application, and explore

its potential in wheat breeding goals. The purposes of this study are to: (i) evaluate the contribution of the integrated application of domain knowledge technologies (supervised fine-tuning, retrieval augmented generation, and reinforcement learning from human feedback) to achieving wheat breeding goals, and analyze the performance of cross-domain data fusion in wheat yield prediction; (ii) explore the response of WBLM in coping with multidimensional breeding goals, and generate personalized decision support from the aspects of phenotyping estimation, environmental stress assessment, target germplasm screening, cultivation technique recommendation, seed price query; (iii) release the study dataset to promote research and application innovation in this field.

## **2. Study area and data**

### *2.1 Experimental sites and design*

The experiment was conducted for two years (2021-2022 and 2022-2023), with 305 and 351 varieties, respectively. The varieties in the second year included the varieties in the first year and 46 varieties were added (Table S1). The experimental sites were set up in Changxing and Yuhang Agricultural Experimental Bases of Zhejiang University Agricultural Experiment Station in Zhejiang Province, China (Fig. 1a, Table S2). Specific planting information is shown in Table S3. The experimental fields were not sprayed with pesticides and herbicides, and weeds were not controlled manually or mechanically. Maintaining the natural growth environment is to develop competitive wheat varieties that have a greater competitive advantage than wheat weeds. The water required for wheat growth comes from natural rainfall. Both places have a subtropical monsoon climate.

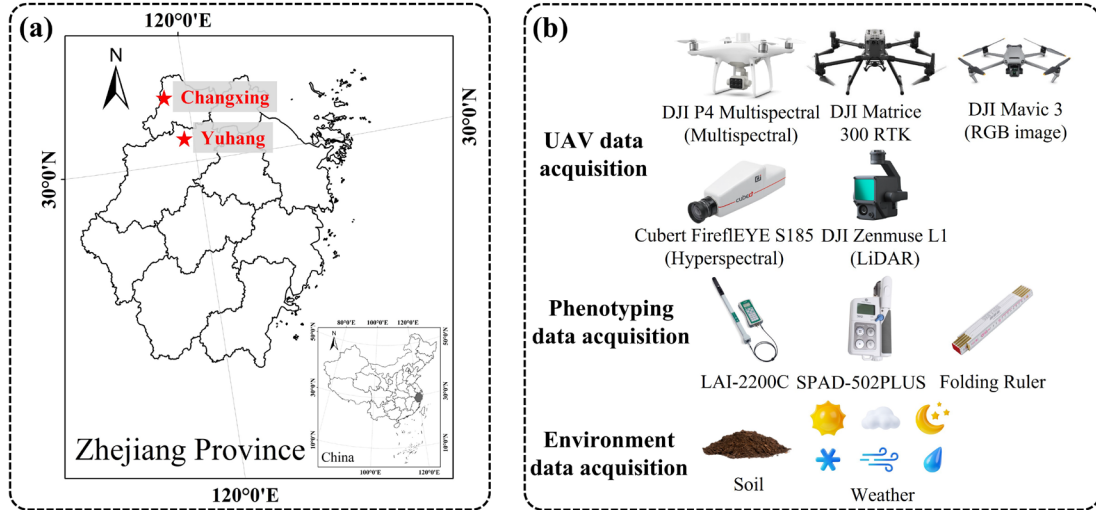


Fig. 1. (a) Experimental sites. (b) Multi-source data acquisition.

## 2.2. Data acquisition

### 2.2.1. UAV data

For the experimental field, we used multiple sensors and multiple UAVs to acquire hyperspectral (HS), lidar, multispectral (MS), and RGB (red, green, blue) data on the same day and compiled them into a RS dataset (Fig. 1b). The Matrice 300 RTK (DJI, China) was selected as the flight platform to carry the Zenmuse L1 (DJI, China) lidar camera and the FirefLEYE S185 (Cubert, Germany) hyperspectral camera to obtain lidar data and HS data respectively. FirefLEYE S185 covers the visible and near-infrared bands from 450 to 950 nm, has 125 spectral channels, and can achieve synchronous frame imaging, spectral resolution: 8 nm @ 532 nm, spectral sampling interval 4 nm. Zenmuse L1 has a range of 190m @ 10%, 100 klx, point cloud data rate multi-echo: maximum 480,000 points/second, elevation accuracy: 5cm @ 50m, plane accuracy: 10cm @ 50m. The Phantom 4 multispectral (DJI, China) and the Mavic 3E (DJI, China) were used to obtain MS data and RGB image respectively. The MS includes five bands, blue: 450 nm  $\pm$  16 nm; green: 560 nm  $\pm$  16 nm; red: 650 nm  $\pm$  16 nm; red edge: 730 nm  $\pm$  16 nm; near infrared: 840 nm  $\pm$  26 nm. The Mavic 3E is equipped with a wide-angle camera 4/3 CMOS, with 20 million effective pixels and a maximum photo size of 5280 $\times$ 3956. The telephoto camera has an equivalent focal length of 162 mm, 12 million pixels, and 56x hybrid zoom.

UAVs were used to collect data during the wheat growth period many times, all under low wind speed and clear and cloudless conditions at noon using different UAVs and sensors. During automatic data collection, the UAV's flight altitude was 15 m, and other flight parameters such as overlap rate were set according to the parameters recommended by the equipment manufacturer. During manual data collection, the Mavic 3E UAV flight altitude was maintained at 3 m and a 7x zoom was set to obtain images and video data of the experimental field. In particular, since the UAV used supports image-free control technology and the experimental field area is relatively small, no ground control points were set and no geometric correction and registration of the data was performed.

### *2.2.2. Phenotypic data*

Phenotypic data collection involves chlorophyll content, leaf area index (LAI), canopy height (CH) and yield (Fig. 1b). Field phenotyping data of wheat were collected six times during 2021-2022 (on January 19, March 8, April 2, April 15, April 29, and May 18, 2022) and nine times during 2022-2023 (on December 27, 2022; February 16, March 4, March 19, April 7, April 22, May 1, May 13, May 19, 2023). UAV RS and phenotyping data were collected on the same day.

The chlorophyll content of the wheat canopy was measured using a SPAD-502 PLUS chlorophyll meter (Konica Minolta, Japan). Five wheat plants with representative growth in each wheat planting plot of the field experiment were randomly selected. For each wheat plant, three leaves without pests and diseases, physiological spots, and mechanical damage were selected, and the tip, middle, and base of each leaf were measured. All the measured values were averaged as the SPAD value of the canopy leaves of the wheat germplasm in the plot. The LAI of the wheat canopy in each plot was measured using a LAI-2000C plant canopy analyzer (LI-COR, USA). Five sampling points with uniform growth were selected at the four corners and the center of each plot, and the LAI values were measured and recorded using a LAI-2200C according to the standard method. Each sampling point was measured three times and the average value was taken as the LAI of the sampling point. We recorded

the average of the LAI of the five sampling points after scatter correction as the LAI of the plot. In each plot, five CH samples were randomly selected for measurement using a tape measure, and the average value was taken as the CH of the plot. The manually measured CH was used to verify the CH derived from the UAV light detection and ranging (lidar) point cloud. Wheat was harvested when mature in each plot. After threshing, the grain from each yield plot was weighed and yield was expressed as  $\text{kg ha}^{-1}$  and standardized to a moisture content of 12.5% (State Administration for Market Regulation and Standardization Administration of the P.R.C, 2023).

### *2.2.3. Environmental data*

The weather data continuously recorded by meteorological equipment at each agricultural experimental base and the meteorological observation station of the China Meteorological Administration were used to provide us with weather data for two-year growing season (Fig. 1b). The data mainly include daily average temperature, dew point temperature, precipitation, net solar radiation intensity, wind speed and other data. The average annual temperature is  $15.6\text{ }^{\circ}\text{C}$ , the average relative humidity is 76%, the annual rainfall is 1309 mm, and the average of 1810 hours of sunlight per year at Changxing Agricultural Experiment Station. The average annual temperature is  $16.2\text{ }^{\circ}\text{C}$ , the average relative humidity is 68%, the annual rainfall is 1400 mm, and the average of 1970 hours of sunlight per year at Yuhang Agricultural Experiment Station.

The test soil was collected before sowing at different locations (0-20 cm) in the experimental field. The collected soil was placed in turnover boxes and then sent for testing in time to determine the physical and chemical properties of the soil. Soil pH = 6.2, total N =  $1.32\text{ g kg}^{-1}$ , available potassium =  $94.9\text{ mg kg}^{-1}$ , available phosphorus =  $1.9\text{ mg kg}^{-1}$  and soil organic C =  $12.4\text{ g kg}^{-1}$  at Changxing Agricultural Experiment Station. Soil pH = 6.14, total N =  $1.68\text{ g kg}^{-1}$ , available potassium =  $187\text{ mg kg}^{-1}$ , available phosphorus =  $63.6\text{ mg kg}^{-1}$  and soil organic C =  $16\text{ g kg}^{-1}$  at Yuhang Agricultural Experiment Station.

### *2.3. Data processing*

### *2.3.1. Data preprocessing*

The acquired UAV data were preprocessed to generate digital orthophoto map (DOM) for subsequent processing according to each plot. Hyperspectral data were converted into reflectance images after radiometric correction using the supporting Cubert Utils Touch software (Cubert, Germany) and radiometric correction plates. Then, Agisoft Metashape (Agisoft, Russia) was used to align photos, create dense point clouds, generate grids, and generate textures to get DOM for subsequent processing. The MS data was imported into Pix4Dmapper (Pix4D, Switzerland) software for initialization processing, point cloud and texture, DSM and DOM generation operations. The irradiance value captured by the light intensity sensor during flight was used to compensate the MS bands for illumination, eliminating the interference of ambient light on data collection. The bands are then radiometrically calibrated using the radiometric calibration plate image acquired simultaneously during data collection. Furthermore, the radiometrically calibrated images were stitched to generate DOM. Finally, the DOM was normalized to obtain reflectance images for subsequent generation of vegetation indexes (VI). The lidar data were processed using DJI Terra (DJI, China) to generate three-dimensional point clouds. The RGB images were imported into Pix4Dmapper to stitch RGB DOM. In addition, one frame of the video obtained by manual flight is extracted every five seconds as an image for storage. These images were divided according to different germplasms (different plots). Then, the wheat heads (WH) in the images were manually annotated to produce a WH dataset.

### *2.3.2. Spectral data processing*

The processed MS and HS bands were used for VIs calculation to analyze the canopy spectral features of different plots. VIs commonly used for phenotyping estimation and grain yield prediction were selected, including NDVI, SAVI, kNDVI, NIRv and PSRI (Table 1).

The fractional vegetation cover (FVC) of the plots, i.e., the percentage of the vegetation area to the plot area (Yang et al., 2022), was calculated as a valuable indicator of crop density and structural information. The vegetation area of the plot was

extracted from the MS image by excluding the background soil using a Transformer-based segmentation algorithm, similar to related study (Cui et al., 2023). The number of vegetation pixels in each plot was then divided by the total number of pixels in that plot to calculate FVC (Maimaitijiang et al., 2020).

### *2.3.3. Lidar data processing*

The CH was extracted from LiDAR point clouds and used as canopy structure features. The bare ground digital elevation model (DEM) was created using point cloud data acquired before the emergence of seedlings in the field. Then, the digital surface model (DSM) representing all objects (vegetation) on the ground was constructed based on the point cloud data acquired at different times. Thus, the CH is obtained by pixel-level subtraction of the generated DSM and DEM (Maimaitijiang et al., 2020). Finally, the obtained lidar data were used to extract CH in different plots in the wheat field.

In addition, the measurement tool of Terra software (DJI, China) was used to mark the reference surface for canopy volume (CV) measurement of each plot based on the lidar point cloud and the boundaries of different plots. The sum of the excavated volume and the filled volume above and below the reference surface is taken as the spatial volume of the reference surface. It should be noted that since there are two types of reference planes, the lowest point (the plane on which it is located) and the average plane, the average value of the volumes obtained from the lowest point and the average plane is taken as the spatial volume of the plot (Table 1).

### *2.3.4. RGB image processing*

To obtain the lodging level of different plots in the wheat field, we refer to a study to construct a wheat lodging area segmentation model (Zhang et al., 2023). Then we use the ratio of the lodging area extracted from the plot to the plot area to determine the plant lodging (PL) level of the plot. In our experiment, the lodging levels were divided into: no lodging (0), slight lodging (0-50%), severe lodging (50-100%), and special (no crop or only a few plants) (Saskatchewan Seed Growers' Association, 2024).

We implemented the detection and counting of WH in the field based on the two-stage method FR-Transformer proposed in our previous study (Zhu et al., 2022) and

RGB images. Then, we used this method to obtain the number of WH in the preprocessed WH images of each plot, and averaged the number of WH in each plot. Finally, the ground coverage area of the WH image was calculated using the UAV flight altitude and camera field of view (Avola et al., 2021), and the number of WH per unit area of the plot was further calculated.

Due to the lack of herbicide spraying and manual weeding, weeds in wheat fields grow randomly and in large numbers. To study the environmental (weed) stress of wheat growth, we focused on the severity of weeds in each plot and the area 10 to 20 cm wide outside the plot in the wheat field. We referred to a study (Anderegg et al., 2023) to extract the number of pixels in the plot and specific area and the number of weed pixels in them, and then used the ratio of the number of weed pixels to the number of pixels in the plot and specific area to classify each plot according to the weed level (WL). The weed level can be roughly divided into: no weeds (0-10%), slight weeds (10-40%), moderate weeds (40-70%), and severe weeds (70-100%).

Table 1. Definition of features extracted from different sensors

Sensor	Features	Formulation	References
MS (Spectral information)	Normalized Difference Vegetation Index	$NDVI = \frac{(NIR - R)}{(NIR + R)}$	(Tucker, 1979)
	Soil-Adjusted Vegetation Index	$SAVI = \frac{(1 + L) \times (NIR - R)}{(NIR + R + L)}, L = 0.5$	(Huete, 1988; Richardson and Everitt, 1992)
	kernel Difference Index	$kNDVI = \tanh\left(\left(\frac{NIR - R}{2\sigma}\right)^2\right)$ , where $\sigma$ is a tunable length-scale parameter intended to capture nonlinear sensitivity of NDVI to vegetation density. If $\sigma = 0.5(NIR + R)$ , which simplifies to $kNDVI = \tanh((NDVI)^2)$ .	(Camps-Valls et al., 2021)
	Near-Infrared Reflectance of Vegetation	$NIR_v = NIR \times NDVI$	(Badgley et al., 2017)

Plant Reflectance Index	Senescence	$PSRI = \frac{(R-G)}{NIR}$ , $R$ , $G$ , and $NIR$ denote the reflectance of the red, green, and near-infrared bands from the 5-band Phantom 4 multispectral, respectively.	(Cao et al., 2019)
HS (Spectral information)	Normalized Difference Vegetation Index	$NDVI = \frac{(NIR-R)}{(NIR+R)}$	(Tucker, 1979)
	Soil-Adjusted Vegetation Index	$SAVI = \frac{(1+L) \times (NIR-R)}{(NIR+R+L)}$ , $L = 0.5$	(Huete, 1988; Richardson and Everitt, 1992)
kernel Difference Index	Normalized Vegetation Index	$kNDVI = \tanh\left(\frac{NIR-R}{2\sigma}\right)$ , where $\sigma$ is a tunable length-scale parameter intended to capture nonlinear sensitivity of NDVI to vegetation density. If $\sigma = 0.5(NIR + R)$ , which simplifies to $kNDVI = \tanh((NDVI)^2)$ .	(Camps-Valls et al., 2021)
	Near-Infrared Reflectance of Vegetation	$NIR_v = NIR \times NDVI$	(Badgley et al., 2017)
	Plant Senescence Reflectance Index	$PSRI = \frac{(R_{680} - R_{500})}{R_{750}}$ , $R_{680}$ , $R_{500}$ and $R_{750}$ denote the reflectance at 680 nm, 500 nm, and 750 nm respectively.	(Cao et al., 2019)
LiDAR (Structural information)	Canopy Height (CH)	$CH = DSM - DEM$	(Maimaitijian et al., 2020)
LiDAR (Structural information)	Canopy Volume (CV)	$CV = \text{Excavated volume} + \text{Filled volume}$ , DJI Terra software (DJI)	<a href="https://enterprisedji.com/dji-terra">https://enterprise.dji.com/dji-terra</a>
RGB image (Structural information)	Plant Lodging (PL)	$PL = \frac{\text{Number of lodging pixels in the plot}}{\text{Total number of the plot pixels}} \times 100\%$	(Zhang et al., 2023)

RGB video	Wheat Head (WH)	WH = The number of wheat head detection	(Zhu et al., 2022)
(Reproduction information)			
RGB image	Weed Level (WL)	WL = $\frac{\text{Number of weed pixels in the plot and specific area}}{\text{Total number of the plot and specific area pixels}} \times 100\%$	(Anderegg et al., 2023)
(Environment al information)			
MS	Fractional Vegetation Coverage (FVC)	FVC = $\frac{\text{Number of crop pixels in the plot}}{\text{Total number of the plot pixels}} \times 100\%$	(Cui et al., 2023)
(Environment al information)			

---

\*  $R$ ,  $G$  and  $NIR$  are the pixel values of the red, green and near-infrared bands, respectively.

#### 2.4. Construction of Cross-domain knowledge base

The cross-domain knowledge base (in Chinese and English) consists of multi-source datasets in the field (Fig. 2a) and external domain knowledge base (Fig. 2b). The multi-source datasets in the field include UAV RS data, phenotyping data, weather data. The external domain knowledge base includes:

(1) wheat germplasm data (22k), mainly including variety name, place of origin, nutritional quality, resistance and agricultural traits. In terms of nutritional quality, key parameters such as crude protein, lysine, and sedimentation value are involved. In terms of resistance, it covers important characteristics such as disease resistance (stripe rust, leaf rust, powdery mildew, etc.), drought resistance, and cold resistance. In addition, agronomic traits such as maturity, plant height, thousand grain weight, and grain hardness are also recorded.

(2) wheat cultivation technique data (10k), covers the entire process from pre-planting preparation to post-harvest storage, mainly including the selection of suitable varieties, soil preparation, sowing, fertilizer management, irrigation and pest and

disease control techniques.

(3) wheat plant protection technique data (10k), mainly including disease prevention and control, pest prevention and control, weed management, as well as new techniques such as precision plant protection based on artificial intelligence and RS, agricultural UAV flight control and green prevention and control.

(4) wheat seed price data (20k), mainly including observation point, variety name, price, specification, planting area and time, etc. For observation points, the economic level and planting demand of different regions lead to price differences; for varieties, different varieties have different characteristics and application scenarios, and high-quality varieties are usually more expensive; different specifications of packaging and planting areas affect the final selling price; prices change over time due to changes in market supply and demand, especially natural disasters or policy adjustments.

The wheat germplasm data comes from the Chinese Crop Germplasm Information Network (<https://www.cgris.net/>). The data on wheat cultivation technique and wheat plant protection technique come from search engines (Google, Bing, Baidu), and the search terms include "wheat cultivation technique, wheat plant protection technique, 小麦栽培技术, 小麦植保技术". The wheat seed price data comes from the National Seed Market Monitoring Information Release Platform (<http://202.127.45.18/>). All data from this study have been made publicly available (<https://doi.org/10.5281/zenodo.13736773>).

### **3. Methods**

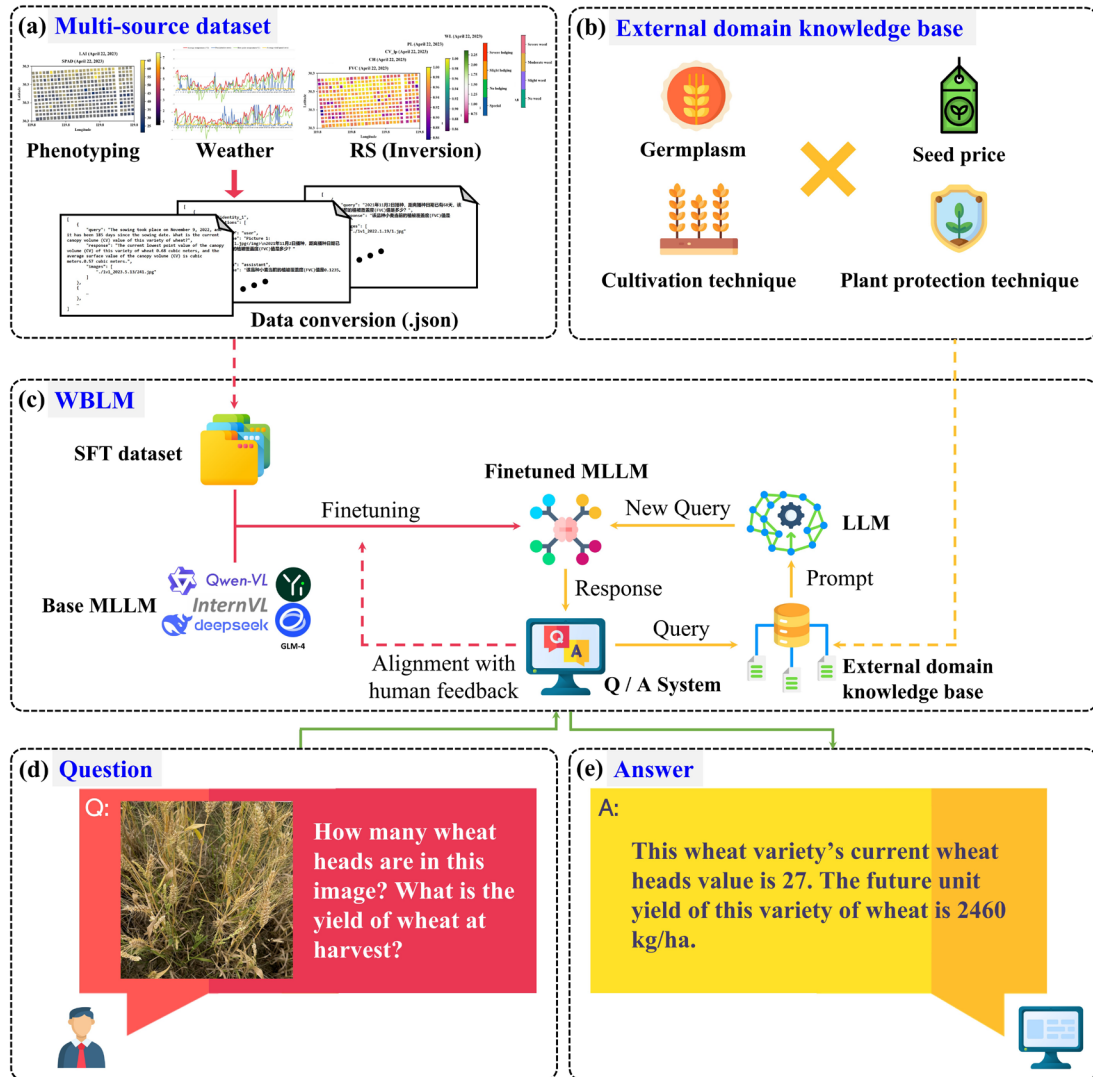


Fig. 2. A workflow for the construction and application of a multimodal large language model for wheat breeding (WBLM). (a) Multi-source dataset construction. (b) External domain knowledge base construction. (c) The WBLM with domain knowledge is constructed using supervised fine-tuning, retrieval augmented generation, and reinforcement learning from human feedback. (d) The user's question (image and text) is sent to WBLM. (e) The WBLM answers the question.

### 3.1. Construction of WBLM

We construct a WBLM with domain knowledge using the supervised fine-tuning (SFT), retrieval augmented generation (RAG) and reinforcement learning from human feedback (RLHF) technologies based on different MLLMs and cross-domain knowledge base. WBLM consists of two parts. The part 1 builds a RAG system based

on the LlamaIndex large model application framework (<https://www.llamaindex.ai/>) and the Milvus vector database (<https://milvus.io/>) (Fig. 2c, yellow line). The part 2 uses STF and RLHF methods to obtain a WBLM that follows breeding preferences (Fig. 2c, red line). We regard the input of part 1 as a query (Fig. 2d), and the original query and the output of part 1 as a new query. The part 2 receives the new query, processes it, and then outputs the result to the Q/A system (Fig. 2e).

To make WBLM better adapt to breeding tasks, we use RAG technology to conveniently and efficiently supplement the knowledge not covered by STF and RLHF methods. First, we convert the data of the files in the external domain knowledge base, use BGE-M3 to generate embedding vectors (J. Chen et al., 2024), and then import the data into the Milvus vector database. Then, LlamaIndex receives user input and initiates a retrieval request to the Milvus database based on the input, using a hybrid retrieval (BGE-M3) and re-ranking (BGE-Reranker-V2-M3) pipeline. LlamaIndex merges the retrieval results with the input to form a new prompt. After that, LlamaIndex inputs the new prompt to InternLM2.5-7B-Chat to achieve reasoning and answer generation based on the retrieved knowledge (Cai et al., 2024).

The training process using the STF and RLHF methods is divided into three stages. In the first stage, we collect demonstration data and train a supervised policy. Based on the cross-domain knowledge base, we artificially construct a question-answering dataset that we hope the model generates aligned answers to SFT the pre-trained MLLM. For questions we want the model to answer well, we collect the answers we want the model to output to increase the probability of the model generating the expected answers. We choose currently popular and competitive open-source MLLMs for model construction and fine-tuning, including Qwen-VL (Qwen-VL-Chat), InternVL (InternVL2-8B and InternVL2-2B), Yi-VL (Yi-VL-6B), Deepseek-VL (DeepSeek-VL-7B-chat and DeepSeek-VL-1.3B-chat) and GLM-4 (GLM-4V-9B), all of which support English and Chinese. It cannot be denied that we mainly provide a method to build an MLLM suitable for wheat breeding, rather than having to choose a specific open-source MLLM, as models with better performance are constantly emerging. We used Scalable lightWeight Infrastructure for Fine-Tuning (SWIFT) to fine-tune the MLLM (The

ModelScope Team, 2024). We refer to the SWIFT recommended training script, in which the LoRA (Low-Rank Adaptation) fine-tuning method is selected, the number of epochs is set to 5, and no further hyperparameter adjustment is performed. All fine-tuning and inference were performed on four V100 NVIDIA GPUs with 32GB. Specifically, dataset  $D$  consists of the model input prompt and the answer that the breeder expects the model to output, denoted by  $x$  and  $y$  respectively. The model is denoted by  $\pi_\theta$ , and the length of  $y$  is  $T$ . When prompt  $x$  is given, the probability that the model generates answer  $y$  can be expressed as formula (1). Where  $\pi_\theta(y_t|x, y_{1:t-1})$  denotes the probability of the model outputting the  $t$ -th token given the input before the  $t$ -th token.

$$\pi_\theta(y|x) = \left[ \prod_{t=1}^T \pi_\theta(y_t|x, y_{1:t-1}) \right] \quad (1)$$

The SFT stage uses the following loss to train the model. For simplicity, we call the model trained in this stage the SFT model.

$$L_{\text{SFT}} = -E_{(x,y) \sim D} [\log \pi_\theta(y|x)] = -E_{(x,y) \sim D} \left[ \sum_{t=1}^T \log \pi_\theta(y_t|x, y_{1:t-1}) \right] \quad (2)$$

The second stage collects comparative data consisting of questions and different answers. Labels indicate their preferred answer given the input. A reward model (RM) is then trained to predict the breeder's preferred answer. Specifically, the model takes prompt and answer as input and outputs a scalar value. We use  $r_\phi$  to denote the RM, and  $r_\phi(x,y)$  denotes the scalar output of the RM given prompt  $x$  and answer  $y$ . The dataset  $D$  used to train the RM consists of the model input prompt, the answer that the breeder wants the model to output, and the answer that the breeder does not want the model to output, denoted by  $x$ ,  $y_w$ , and  $y_t$  respectively. We are given data  $(x, y_w, y_t)$ , and use the maximum likelihood estimation loss to train the RM.  $\sigma$  denotes the sigmoid function. During training,  $K$  answers are selected each time and combined in pairs.

$$L_R(r_\phi) = -E_{(x,y_w,y_t) \sim D} [\log \sigma(r_\phi(x, y_w) - r_\phi(x, y_t))] \quad (3)$$

In the third stage, proximal policy optimization (PPO) is used to optimize the policy

for the RM. We use the output of the RM as a scalar reward and use the PPO algorithm to fine-tune the SFT model to optimize this reward (Schulman et al., 2017). Among them, the second and third stages can be carried out iteratively. We collect more comparison data on the current best policy, use it to train a new RM, and then train a new policy. In practice, most of our comparison data comes from supervised policies, and some of it comes from PPO policies. After training the RM, we have obtained an approximate reward function. Consider the model as a policy in the reinforcement learning (RL) problem, and the input and output of the model can be regarded as the state and action of RL respectively. We can use RL algorithms to train the model and train the model to output the answer with the highest reward. However, the RL training process is very unstable, so the SFT model is used as a reference model, denoted by  $\pi_{\text{ref}}$ . The KL divergence regularization term with the reference model is added to the objective function (4) to limit the update range of the model. Among them, the hyperparameter  $\beta$  controls the degree of deviation from the reference model.

$$J_{r_\phi}(\pi_\theta) = E_{x \sim D, y \sim \pi_\theta} [r_\phi(x, y)] - \beta D_{KL}(\pi_\theta(y|x) | \pi_{\text{ref}}(y|x)) \quad (4)$$

According to the objective function (4), the KL divergence term is expanded, and the final comprehensive reward is:

$$r(x, y) = r_\phi(x, y) - \beta(\log \pi_\theta(y|x) - \log \pi_{\text{ref}}(y|x)) \quad (5)$$

The objective function is:

$$J_{r_\phi}(\pi_\theta) = E_{x \sim D, y \sim \pi_\theta} [r(x, y)] \quad (6)$$

We created three different datasets: (1) The SFT dataset (75k) is created using multi-source datasets from the field, which contains questions and answers for training the SFT model. 80% of this dataset is used for training, and 20% is used for accuracy testing of wheat breeding model evaluation benchmark (phenotyping estimation task and environmental stress assessment task). (2) The RM dataset, with breeder rankings of model outputs, is used to train the RM. (3) The PPO dataset, without any breeder labels, which are used as inputs for RLHF fine-tuning. External domain knowledge base is mainly used by RAG methods. The dataset format refers to SWIFT (Table S4).

### 3.2. *WBLM evaluation benchmark*

In order to comprehensively evaluate the performance of MLLM in scientific breeding work, it is necessary to build a standardized machine and human evaluation benchmark. This benchmark aims to integrate challenges from various wheat breeding tasks. This benchmark aims to integrate challenges from various wheat breeding tasks. We have specifically designed many professional Chinese and English questions on wheat breeding and corresponding standard answers, covering five tasks: phenotyping estimation, environmental stress assessment, target germplasm screening, cultivation technique recommendation, and seed price query. The phenotyping estimation includes seven subtasks (Yield, SPAD, LAI, CH, CV, WH and PL), the environmental stress assessment includes two subtasks (WL and FVC), the target germplasm screening includes five subtasks: high quality (HQ), disease resistance (DS), drought resistance (DR), maturity period (MP), adapt to mechanized (AM), the cultivation technique recommendation includes two subtasks: cultivation technique (CT) and plant protection technique (PPT), and the seed price query includes one subtask seed price (SP) query. Through objective evaluation indicators and manual scoring and sorting, the evaluation team conducted a detailed evaluation of the answers of multiple MLLMs including WBLM, covering three aspects: accuracy, stability, and reasoning.

#### (1) Accuracy

We evaluate different subtasks under five tasks, respectively. For the phenotyping estimation task and the environmental stress assessment task, the RMSE and  $R^2$  evaluation indicators are selected for regression tasks (estimating the values of FVC, SPAD, LAI, CH, CV, WH, and Yield), and the accuracy evaluation indicator is selected for the classification task (estimating the categories of WL and PL). For each subtask under the target germplasm screening task and cultivation technique recommendation task, each MLLM is tested multiple times (1k), and each test is manually judged whether the answer is correct. Then the proportion of the number of correct answers to the total number of tests is used as the evaluation indicator. For the seed price query task, we counted whether each result after multiple (1k) tests was consistent with the data in the knowledge base (price  $\pm 10\%$ ), and took the proportion of the total number

of consistent data to the total number of tests as the evaluation indicator.

### (2) Stability

We evaluate the consistency and robustness of the answers. The evaluation indicator of stability is the proportion of times that satisfy the stability requirements in the total number of tests (1k), where the stability requirement is that the deviation of the numerical value in the answer is within  $\pm 10\%$ , and whether the text satisfies the requirement is manually judged. Consistency: Since cross-domain data are related, the answers given after inputting different data from cross-domain data into the model should remain basically consistent. Robustness: The model's answer or performance should not change significantly when faced with small changes in input data. Robustness requires that the model should have a certain degree of fault tolerance.

### (3) Reasoning

We evaluate the logical deduction, inductive reasoning, and explanation of the answers. The evaluation indicator of reasoning is the proportion of the total reasoning score of a single model after multiple tests (1k) to all scores. After one test,  $x$  MLLM models output  $x$  answers. After manually analyzing  $x$  answers, we select a score from 1 to  $x$  points for each answer and the score can only be selected once until all answers are scored. We sum up the answer scores of different models after multiple tests as the total reasoning score of the corresponding model. Then calculate the proportion of the total reasoning score of different models to all scores  $((1 + x) * x / 2)$ . Logical deduction: The model can deduce new conclusions or answers through logical reasoning based on known facts, rules and conditions. This requires the model to understand the logical relationships in the question and accurately apply these relationships to deduce answers. Inductive reasoning: The model can summarize general rules or patterns from a series of specific examples or observations and give reasonable answers based on them. Inductive reasoning requires the model to have the ability to abstract and generalize information. Explanation: The reasoning process is explained or visualized to a certain extent to help user understand the source and basis of the answer.

## **4. Results and Discussion**

#### 4.1. Evaluation of WBLM

The newly constructed wheat breeding model evaluation benchmark was used to evaluate closed-source MLLMs (Qwen 2.5, ERNIE Bot 4 Turbo, GPT-4o Plus and Gemini Pro 1.5, abbreviated as Qwen, ERNIE Bot, ChatGPT, Gemini) and WBLMs built based on different open-source MLLMs (Qwen-VL, InternVL, Yi-VL, Deepseek-VL and GLM-4) (Fig. 3-5, Table S5).

Accuracy evaluation: On various tasks of the evaluation benchmark, the comprehensive performance of WBLM based on InternVL2-8B is better than that of WBLM built on other open-source MLLMs, and is significantly better than closed-source ChatGPT, Gemini, and Qwen. Among them, for LAI evaluation, the  $R^2$  based on InternVL2-8B is 0.795 and the RMSE is 1.302. The  $R^2$  and RMSE of other open-source MLLMs range from [0.674, 0.772] and [1.542, 2.486], and the  $R^2$  and RMSE of closed-source MLLMs range from [0.118, 0.142] and [3.61, 3.985], respectively. ChatGPT shows leading performance among open-source models, although still far behind the WBLM based on InternVL2-8B. In addition, we find that consistent with existing study (Z. Chen et al., 2024), the performance of MLLMs with small parameters in the same series is lower than that of MLLMs with larger parameters, such as InternVL2-8B and InternVL2-2B. We attribute this modest decline to the smaller size of the MLLMs.

Stability evaluation: Compared with closed-source MLLMs, WBLMs based on open-source models outperform in stability tests. Specifically, the WBLM based on InternVL2-8B achieved the best performance in consistency, with a stability score of 0.811, while the stability score of the lowest-performing Qwen 2.5 was only 0.053. The robustness scores of closed-sources MLLM ([0.829, 0.895]) are higher than those of WBLM based on open-source MLLM ([0.735, 0.802]), because closed-source MLLM cannot accurately answer relevant breeding questions in most tasks, and the answers are still wrong and similar when faced with slight changes in input data. However, among multiple WBLMs based on open-source MLLM, WBLM based on InternVL2-8B has a higher robustness score.

Reasoning evaluation: The WBLM based on InternVL2-8B outperforms other MLLMs in logical deduction and explanation evaluation, with the highest scores of 0.158 and 0.15, respectively. The WBLM based on GLM-4V-9B-chat outperforms other MLLMs in inductive reasoning evaluation, with the highest score of 0.16. Compared with accuracy and stability evaluation, reasoning evaluation tests the model's breeding decision support and problem-solving capabilities more. Excellent reasoning ability can enhance users' trust in MLLM and improve user satisfaction (J. Li et al., 2024).

InternVL2-8B based WBLM shows leading performance in most benchmark tests (Fig. 3-5, Table S5). However, the closed-source commercial MLLMs used in this study encountered significant difficulties in the wheat breeding evaluation benchmark test and performed poorly. The main reason is that closed-source commercial MLLM lacks domain knowledge related to wheat breeding, while open-source MLLM obtains it using a combination of domain knowledge technologies (Ming and Li, 2024). Although closed-source MLLMs represented by ChatGPT achieved better performance on the popular MLLM evaluation benchmarks (Fu et al., 2024; Y. Liu et al., 2024; Yue et al., 2024), we did not build WBLM based on closed-source MLLMs because these MLLMs do not support further implementation of the process of this study. If closed-source MLLMs support richer fine-tuning and downstream task customization, they may gain greater commercial value and more users. Although all open-source MLLMs can handle multimodal tasks, different network architectures have different abilities to solve semantic alignment between modalities when integrating visual and textual data, thus affecting the accuracy of the final results. In addition, different training processes, tricks, and private training data are also important factors affecting model performance (D. Huang et al., 2024). In the future, researchers can build breeding models based on MLLM with better performance to provide stronger breeding assistance efficiency and results.

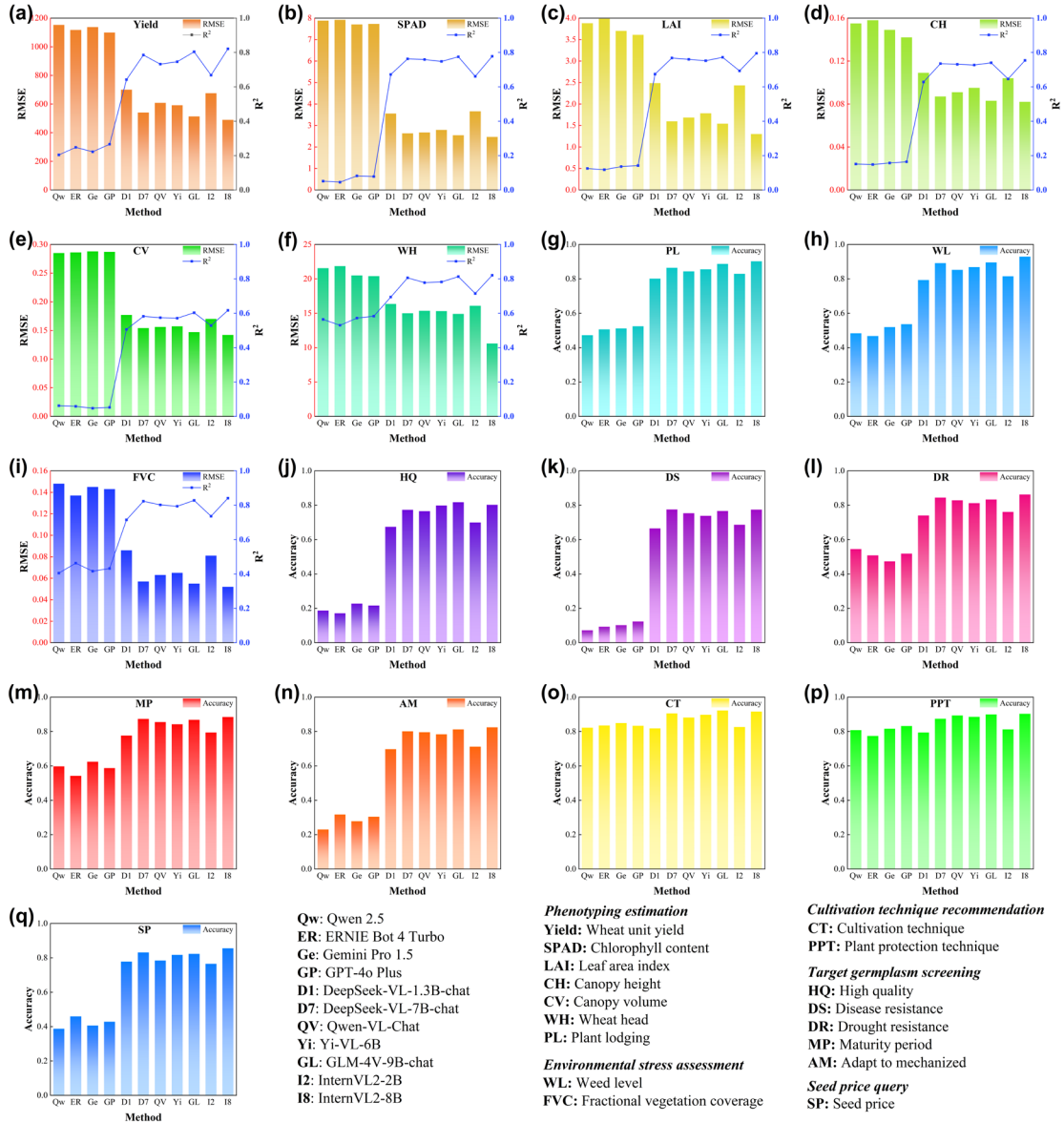


Fig. 3. Comparison of different MLLMs on the evaluation benchmark (accuracy).

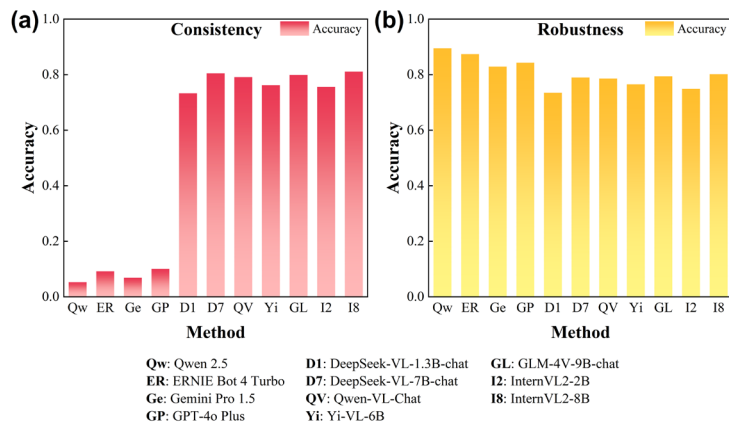


Fig. 4. Comparison of different MLLMs on the evaluation benchmark (stability),

which includes consistency and robustness.

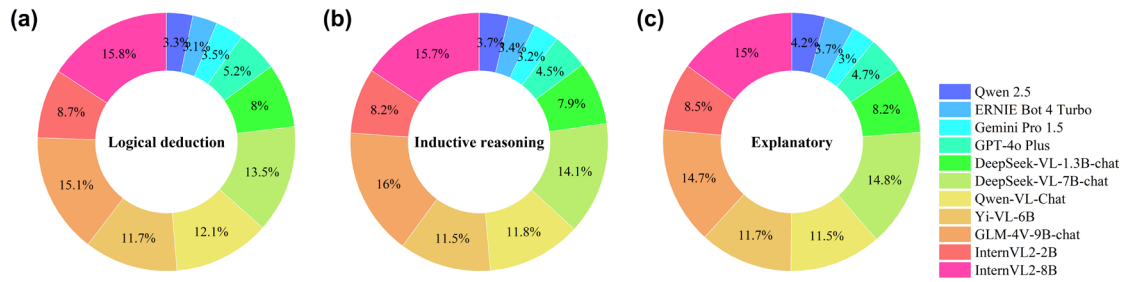


Fig. 5. Comparison of different MLLMs on the evaluation benchmark (reasoning).

This figure shows the total reasoning score as a proportion of all scores after multiple tests of a single MLLM.

## 4.2. Impact of domain knowledge on breeding goals

### 4.2.1. Contribution of the combination of domain knowledge and technology to breeding goals

We evaluated WBLM on the wheat breeding model evaluation benchmark and observed strong performance of WBLM based on InternVL2-8B. In this section, we conduct ablation experiments to test the performance of different domain knowledge technologies combinations in different tasks (Fig. 6 and Table S6).

For the phenotyping estimation task, Yield, SPAD, LAI, CH, and CV show poor performance under the MLLM-only method due to the same lack of domain knowledge. Compared with the MLLM-only method, the MLLM and SFT method, the MLLM and RAG method, and the MLLM and RLHF method all greatly improve the prediction performance of these subtasks. Additionally, for the WH and PL subtasks, MLLM has certain detection and classification capabilities. With the addition of SFT, RAG, and RLHF technologies, the performance is further improved to achieve relatively high  $R^2$  and low RMSE. For the environmental stress assessment task, the results showed that accurate classification of WL was simpler than specific values estimation of FVC. When the method combining MLLM, SFT, RAG, and RLHF was used, the best performance for WL prediction was 0.929 (accuracy), and the best performance for FVC prediction was 0.841 ( $R^2$ ) and 0.052 (RMSE).

When only MLLM is used, the prediction results for the target germplasm

screening task and the seed price query task are poor. The main reason is that the MLLM lacks domain knowledge and price dynamic data, so it cannot answer accurately. Furthermore, the results show that when the MLLM is combined with one or more domain knowledge technologies (SFT, RAG, RLHF), better prediction performance can be achieved. For the cultivation technique recommendation task, because the MLLM has been trained with many images and texts from various data sources, and some wheat cultivation technique knowledge is also covered, thus it can answer some questions well. It is undeniable that when one or more domain knowledge technologies (SFT, RAG, RLHF) are combined, the cultivation technique recommendation is more accurate and the data is traceable.

The method combining MLLM, SFT, RAG and RLHF performs better in different subtasks of the five tasks. It is worth mentioning that by analyzing the prediction results of the above tasks, it can be clearly found that hallucination exists when only the MLLM method is used, which directly reflects the necessity of combining MLLM with domain knowledge technology. With the increase of domain knowledge technology, the  $R^2$  of the methods in the phenotyping estimation and environmental stress assessment tasks gradually increased, and the RMSE decreased. Simultaneously, the consistency of the prediction results in the target germplasm screening, cultivation technique recommendation, and seed price query tasks gradually increased. This shows that all methods based on domain knowledge technology can enhance the model's understanding of specific fields to some extent, improve data interpretation capabilities, and thus optimize prediction accuracy and reliability.

However, when the task involves many rare or long-tail scenarios (e.g., phenotyping estimation tasks), the method combining MLLM, SFT and RLHF outperforms the method combining MLLM, RLHF and RAG and the method combining MLLM, SFT and RAG. When the task involves obtaining knowledge from many structured and domain-related data (e.g., the seed price query task), the method combining MLLM, RLHF and RAG and the method combining MLLM, SFT and RAG outperform the method combining MLLM, SFT and RLHF. This may be due to the unique advantages of different domain knowledge technologies in dealing with specific

tasks. This result is consistent with previous studies (Balaguer et al., 2024; Giuffre et al., 2024; J. Li et al., 2024), which showed that SFT directly optimizes model output by annotating data, RAG integrates external multimodal knowledge to improve answer quality, and RLHF iteratively optimizes generated content to improve task orientation and adaptability. Therefore, the method combining MLLM, SFT, RAG, and RLHF combines the advantages of different technologies to achieve better performance. It should be noted that this method may be affected by the update frequency and accuracy of the knowledge base, resulting in a decrease in the quality of answers (Siriwardhana et al., 2023). In addition, RLHF requires a large amount of interaction data to optimize the MLLM, and sample efficiency issues may occur in the process (Yuan et al., 2024). Future study can integrate more advanced domain knowledge technologies (e.g., knowledge graphs) to extract better domain knowledge to achieve more accurate generation prediction capabilities for different breeding tasks.

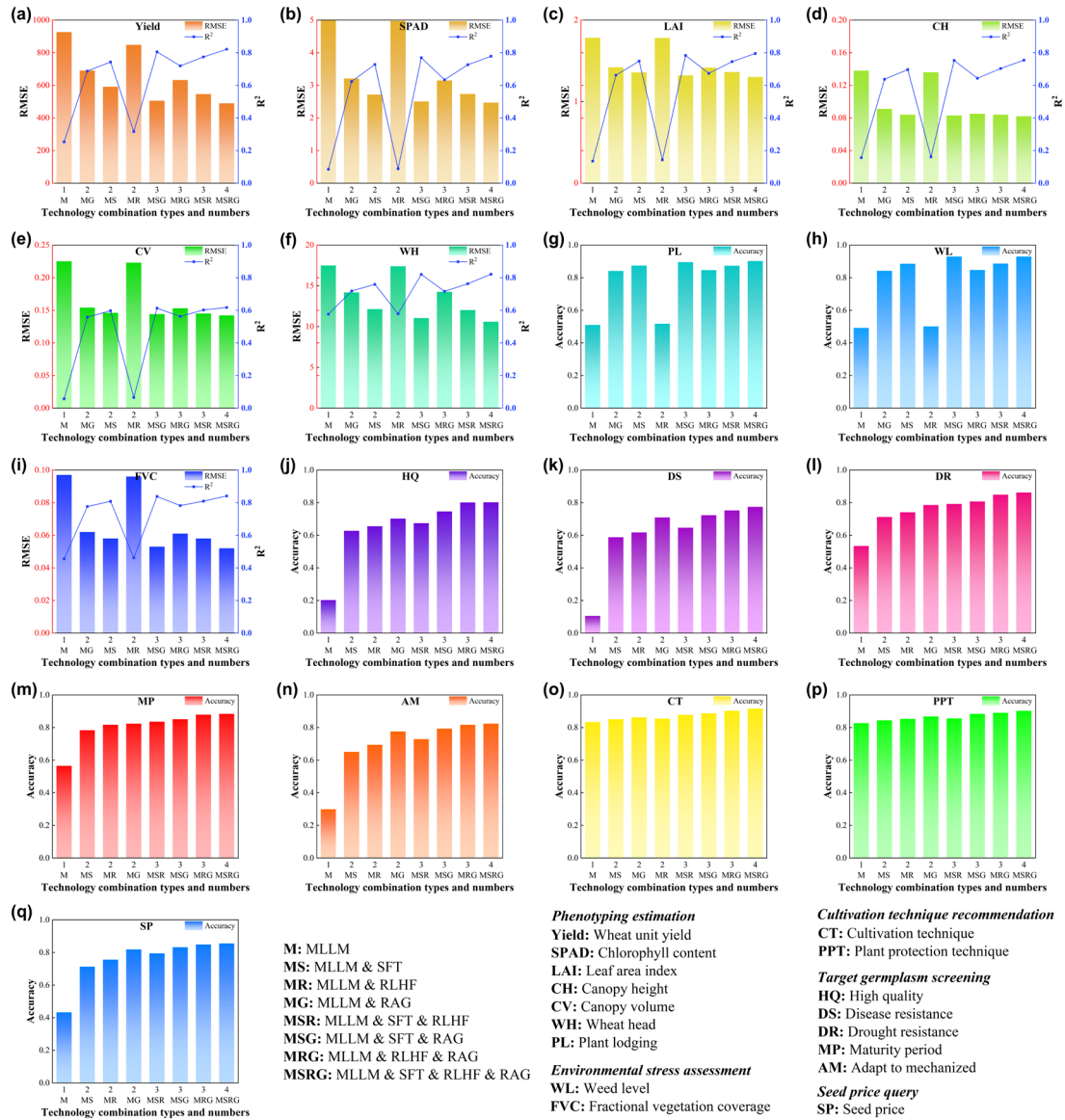


Fig. 6. Prediction performance of different tasks for methods with different combinations of domain knowledge technologies.

#### 4.2.2. Performance of cross-domain data combination in wheat yield prediction

When only RS data is used, the  $R^2$  of wheat yield prediction is 0.707 and the RMSE is 599.532 kg/ha (Fig. 7 and Table S7). The RS data comes from processed data from different UAV sensors. As shown in many previous studies, different information such as VI (spectral), FVC (environment), CH (canopy structure) have become the most commonly used RS indicators in crop yield prediction due to their stable and superior performance (Roth et al., 2022; Skobalski et al., 2024; T. Xu et al., 2023). However, a wide range of environmental conditions such as growing soil, water availability and

atmospheric conditions, as well as different germplasm genes of wheat, also have a significant impact on yield, which may reduce model performance.

The combination of RS and phenotyping data can significantly improve the prediction accuracy compared with using RS data alone. The canopy structure features (LAI) and physiology and biochemistry features (SPAD) obtained from phenotyping data contain independent information about canopy growth and structure, as well as information that indirectly reflects the relative content of current chlorophyll in plant leaves. Furthermore, phenotyping data have the advantage of higher accuracy to a certain extent, and can directly capture more subtle changes and differences, which is particularly important for accurately assessing wheat growth conditions and predicting yields. Therefore, the combination of RS and phenotyping data can improve the prediction accuracy. Many previous studies have verified the potential of coupled RS and phenotyping information in crop yield prediction (Duan et al., 2017; Jin et al., 2024). The combination of RS and weather data slightly improved the prediction accuracy compared with RS data alone, with an increase of 0.014 in  $R^2$  and a decrease of 9.84 kg/ha in RMSE. The information from weather data tends to add supplementary information to RS information in wheat yield prediction, but to a lesser extent than the information contained in phenotyping data. It shows that RS information and weather information at different growth stages are prone to information overlap, further affecting the prediction ability. When the relevant information based on germplasm data (high yield, HQ, DS, DS, MP and AM) was added to the information from RS data, the prediction accuracy of all methods was slightly improved. It shows that using macro-growth conditions provided by RS data and micro-genetic traits provided by germplasm data can provide a more comprehensive assessment of crop growth potential and yield.

The yield prediction performance from the combination of RS, phenotyping, and weather data; RS, phenotyping, and germplasm data; and RS, weather, and germplasm data is better than the combination of the two data types, with  $R^2$  varying from 0.734 to 0.808 and RMSE ranging from 494.967 kg/ha to 572.755 kg/ha. These results indicate that RS, phenotyping, weather, and germplasm information provide unique and complementary information that is helpful for wheat yield prediction. These results at

least partially further explain the benefits of using cross-domain data in wheat yield prediction. For this benefit, we further utilized all the data obtained (RS, phenotyping, weather, germplasm), and the results showed that the yield prediction performance was the best, with an  $R^2$  of 0.821 and an RMSE of 489.254 kg/ha. Related studies have also shown that using one or more data from RS, environment and germplasm can improve the performance of model yield prediction (Feng et al., 2024; Maimaitijiang et al., 2020; Tian et al., 2022). These studies use data fusion as one of the data-level solutions to improve the accuracy of yield prediction. It is undeniable that as the data scale increases, the model can usually achieve improved performance, but this increases the complexity of the model, requiring more powerful computing resources and more complex algorithms (J. Li et al., 2024). And data quality and missing issues directly affect the prediction accuracy of the model (Yang et al., 2023). In addition, obtaining high-quality yield data requires a lot of field experiments and data processing, which increases the cost of data acquisition (Ruan et al., 2022). Although data fusion can improve the generalization ability of the model, the model may still experience performance degradation when facing a completely new planting environment or germplasm (Gu et al., 2024).

The predicted values of wheat yield obtained by the methods (trained using data from different data sources) were compared with the corresponding observed values using the scatter plot (Fig. 7). As expected from the comparable  $R^2$  and RMSE values, the values obtained by the method trained only with RS data are widely scattered on both sides of the regression line, while the values obtained by the method trained with all multi-source data are closely around the regression line. It is worth noting that the data from the China Rural Statistical Yearbook show that the yield per unit area of wheat in Zhejiang Province in 2022 is 4230.2 kg/ha (National Bureau of Statistics of China, 2022), where the points to the right of the purple dashed line in Fig. 7 represent germplasms that exceed the yield per unit area. The germplasms with yields exceeding 4230.2 kg ha<sup>-1</sup> are from China, Japan, Argentina, Italy, Turkey, and Australia. These germplasms showed higher FVC, CH, CV, and WH compared to other germplasms. It should be emphasized that these germplasms achieved higher yields in an environment

with stronger weed competition, thus indicating that these germplasms have stronger competitiveness and adaptability. These wheat germplasms are more valuable in production because their growth shows a certain degree of freedom from weed control activities, reducing production costs and improving yield sustainability.

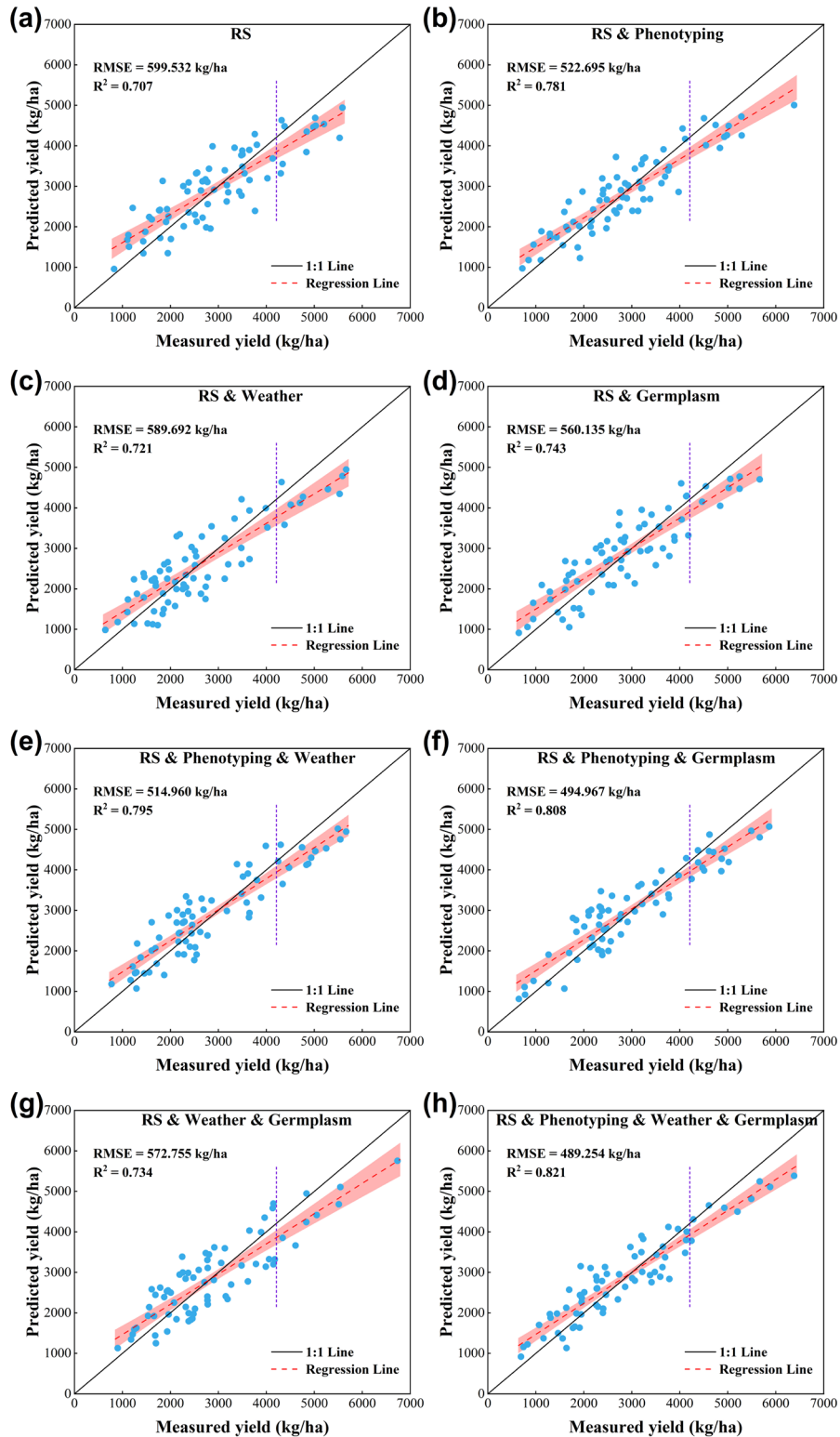


Fig. 7. Cross-validation scatter plot of measured and predicted wheat yield. The black solid line indicates a 1:1 relationship. The blue points to the right of the purple dashed line represent germplasms with wheat yields exceeding 4230.2 kg ha<sup>-1</sup>.

### 4.3. Breeding goals response to WBLM

We compare WBLM with the easily accessible MLLM: Qwen 2.5, ERNIE Bot 4 Turbo, GPT-4o Plus, and Gemini Pro 1.5 in different scenarios (the five tasks of this study) to explore wheat breeding goals response capabilities of MLLM. Since our WBLM and all other MLLMs support both Chinese and English, we chose Chinese and English for testing. The results show that WBLM, Qwen and ChatGPT can correctly and automatically adjust to the corresponding language to answer according to the user's query language, while the other two MLLMs need to explicitly specify the answer language. We aim to demonstrate the practicality and versatility of WBLM and other MLLMs in real breeding applications, providing analysis and insights from the perspective of actual user experience whenever possible.

We can use WBLM and commercial MLLMs to estimate the yield of different germplasms (Fig. 8). Specifically, we provide different phenotyping images and related growth information. Except for WBLM, other MLLMs cannot answer the questions accurately, and WBLM's answers are simple and direct. Some MLLMs cannot answer correctly, but ideas and methods are provided to further answer the question. The results show that WBLM has unique and superior capabilities in yield phenotyping estimation than other MLLMs.

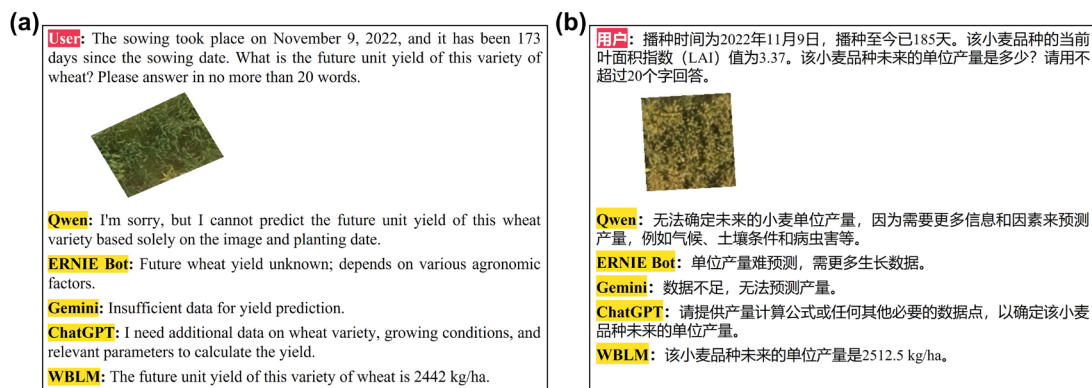


Fig. 8. Examples of phenotyping (yield) estimation on different MLLMs.

We can use WBLM and commercial MLLMs to screen target germplasm. We test five target germplasm characteristics: HQ, DS, DR, MP, and AM, either individually or in combination. Regarding the screening of AM (plant height) (Fig. 9a), Qwen and ERNIE Bot were unable to answer correctly, while other MLLMs were able to answer correctly. For the HQ screening (Fig. 9b), Qwen and ERNIE Bot cannot correctly answer the specific variety name and preservation organization, while other MLLMs can answer correctly. For the MP and AM screening (Fig. 9c), we found that except for Gemini, other MLLMs can correctly output specific wheat variety names that satisfy the requirements. For DS, DR and HQ screening (Fig. 9d), each MLLM can correctly output specific wheat varieties. Analyzing the above results, except for WBLM, which has a clear data source, the data sources of other MLLMs are unknown. In addition, the answers of different MLLMs vary greatly, so users need to verify and refer to them with caution. In addition, if MLLM cannot answer the question correctly by self-judgment, some solutions or methods will be provided.

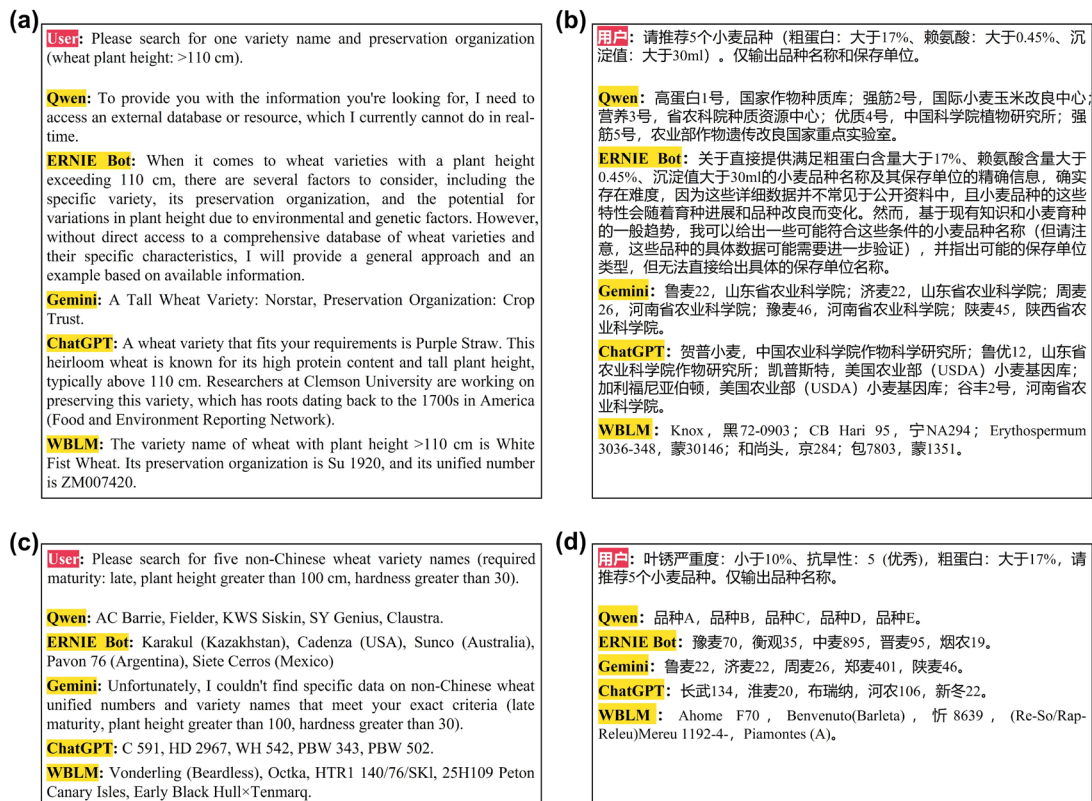


Fig. 9. Examples of target germplasm screening on different MLLMs.

We can use WBLM and commercial MLLMs to assess the environmental stress

(FVC and WL) of different germplasms (Fig. 10). Only WBLM can accurately output the value of FVC and the level of WL. ChatGPT can answer questions in the environmental stress assessment, but the answers are inaccurate. ERNIE Bot and Gemini can only partially answer and the answers are inaccurate. Qwen cannot answer either. Furthermore, we found that when there was no word limit on the answer, WBLM had a deeper understanding of the knowledge in the field of wheat breeding and the answers were more focused and specific.

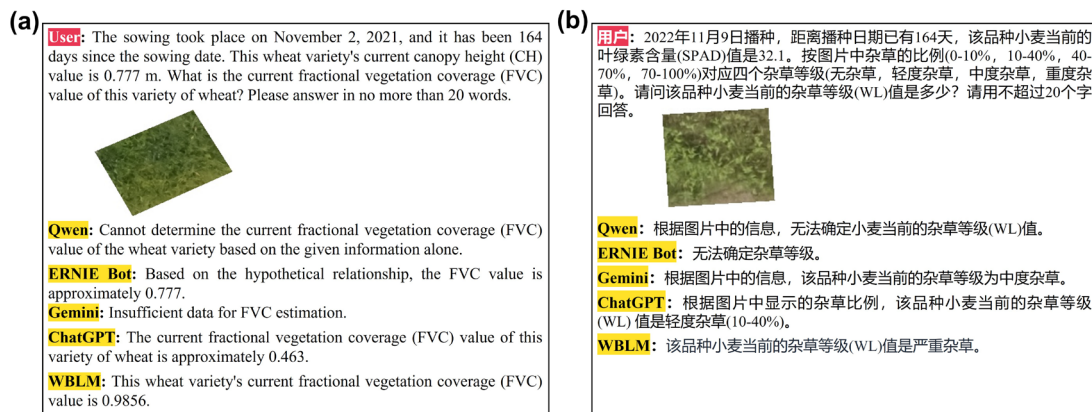


Fig. 10. Examples of environmental stress assessment on different MLLMs.

We can use WBLM and commercial MLLMs to recommend efficient, innovative and sustainable PT and PP techniques (Fig. 11). Focus on their ability to accurately answer questions under different techniques, different growth stages, and different growth environments. The scope of the recommendation: From soil preparation technique before wheat planting, to wheat sowing time, sowing amount and depth; from wheat fertilization management (base fertilizer), to when to apply topdressing and what fertilizer to use; from how to effectively control weeds in field management, to wheat disease and pest control in specific growth periods; from introducing wheat soil testing and formulation technique, to introducing wheat “one spray and three preventions” technique. The results show that the performance of WBLM is on par with Qwen and ChatGPT, and slightly better than the answers of other MLLMs. This reflects WBLM's superior understanding and reasoning of PT and PP technique, resulting in better recommendation results than the answers of other MLLMs.



Fig. 11. Examples of cultivation technique recommendation on different MLLMs.

We can use WBLM and commercial MLLMs to query the seed varieties, specifications and prices at a specified observation point and time (Fig. 12). It can be seen that except for WBLM, none of them can provide accurate answers. Other MLLMs choose to give factors that affect wheat seed prices and suggest methods to obtain relevant data. Through this experiment, we found that for highly dynamic information such as price data, MLLMs need to rely on external data sources to ensure the real-time and accuracy of the data. Although MLLMs can provide trend analysis, principle explanations, or forecasting methodologies based on historical data, they are unable to capture new market conditions, stock prices, commodity prices, or other information that requires real-time updates. Real-time and price data are usually collected and published by specialized financial data providers, market analysis companies or government statistics departments. These data often need to be obtained through subscription services, API interfaces or public market reports.

<p>(a)</p> <p><b>User:</b> Address: Miyun District, Beijing, Time: 2024-06-01, Please answer the price (CNY/bag), variety, and specifications (CNY/bag) of wheat seeds?</p> <p><b>Qwen:</b> I don't have real-time data access for specific local market prices, including wheat seed prices in Miyun District, Beijing, on June 1, 2024. To get accurate information about wheat seed prices, varieties, and specifications, you can follow these steps: Local Agricultural Supply Stores, Agricultural Cooperatives, Online Platforms, Government Resources. If you need general information about common wheat seed varieties and typical prices as of my last update in 2023, I can provide that. However, please note that actual prices may vary significantly due to factors such as market demand, supply, and weather conditions. Would you like me to provide this general information instead?</p> <p><b>ERNIE Bot:</b> As an AI language model, I do not have access to real-time market prices or specific product information for individual businesses or regions. However, I can provide you with a general overview of wheat seed prices, varieties, and specifications in China, which may vary depending on factors such as market conditions, quality, and the specific variety.</p> <p><b>Gemini:</b> Agricultural product prices, including wheat seeds, can fluctuate based on various factors such as seasonality, supply and demand, and specific varieties. To obtain the most accurate and up-to-date information regarding the price, variety, and specifications of wheat seeds in Miyun District, Beijing, for June 2024, I recommend consulting the following resources: Local Agricultural Departments, Seed Retailers and Distributors, Online Agricultural Marketplaces. By utilizing these resources, you can gather the most reliable and relevant information regarding wheat seed prices, varieties, and specifications in Miyun District, Beijing, for June 2024.</p> <p><b>ChatGPT:</b> The price of wheat seeds can vary depending on the variety and specifications, as well as the supplier. For a specific location like Miyun District, Beijing, and a particular date, it's best to consult local agricultural suppliers or seed companies for the most accurate and up-to-date information.</p> <p><b>WBLM:</b> Price: 150 CNY/bag, Variety: Nongda 3486, Specification: 25 kg/bag.</p>	<p>(b)</p> <p><b>用户:</b> 地点: 四川成都市, 时间: 2024-07-24, 请仅回答价格, 品种, 规格是 (小麦种子)?</p> <p><b>Qwen:</b> 对于具体的小麦种子的价格、品种和规格信息, 这些数据通常会根据市场情况、供应商以及具体的品种而有所不同。在现实中, 这类详细信息往往需要通过当地的农业合作社、种子销售商或者官方农业部门来获取。</p> <p><b>ERNIE Bot:</b> 针对您提出的关于2024年7月24日在四川成都市小麦种子的价格、品种及规格的问题, 由于市场价格受多种因素(如供需关系、季节变化、政策调整、种植技术更新等)影响, 且这些信息是实时变动的, 我无法直接提供精确的实时数据。</p> <p><b>Gemini:</b> 很抱歉, 我无法为您提供精确到2024年7月24日, 四川成都市小麦种子价格、品种和规格的具体信息。</p> <p><b>ChatGPT:</b> 在2024年7月24日, 四川成都市的小麦种子价格和品种信息如下: 品种: 常见品种有“川麦”“郑麦”“南麦”等适合四川种植的优质小麦。规格: 一般袋装, 规格为50公斤一袋。价格: 平均价格在200元至400元每袋不等, 具体价格根据品种、质量和市场波动可能有所变化 (China Seed Business) (National Bureau of Statistics)。如需更详细的供应商信息和实时报价, 建议联系当地种子销售商或相关农资市场。</p> <p><b>WBLM:</b> 科成麦4号, 2.5公斤/袋, 25元/袋。</p>
--	--

Fig. 12. Examples of seed price query on different MLLMs.

## 5. Conclusion

In this study, we innovatively applied MLLM to wheat breeding and explored its

potential for application in wheat breeding objectives. Based on different pre-trained open-source MLLMs, we used SFT, RAG, and RLHF technologies to inject cross-domain knowledge into MLLMs, thereby constructing multiple WBLMs. Among them, the WBLM constructed using SFT, RAG and RLHF technologies and InternVL2-8B has leading performance on the evaluation benchmark newly created in this study. The WBLM has competitive advantages over leading proprietary MLLMs, especially in wheat breeding tasks. Then, subsequent experiments were conducted using the WBLM. Ablation experiments indicated that the combination of SFT, RAG, and RLHF technologies can improve the overall generation performance, enhance the generated quality, balance the timeliness and adaptability of the generated answer, and reduce hallucinations and biases. The WBLM performed best in wheat yield prediction using cross-domain data (RS, phenotyping, weather, germplasm) simultaneously, with  $R^2$  and RMSE of 0.821 and 489.254 kg/ha, respectively. Furthermore, the performance of WBLM and other MLLMs for wheat breeding goals was compared from a qualitative perspective of answer generation, and it was found that WBLM could generate more professional decision support answers. This study aims to provide an intelligent and integrated solution for wheat breeding goals, to help breeding work be carried out efficiently, to accelerate the breeding process of excellent varieties, and to provide scientific basis and technical support. In future, we will continue to explore deeper data fusion technology, optimize the generalization ability of the model, and enhance the interpretability of the model to ensure the transparency and reliability of breeding decisions. We will also expand the scope of application of the model to cover more crop varieties and environmental conditions to meet the breeding needs of different regions.

### **CRedit authorship contribution statement**

**Guofeng Yang:** Methodology, Data curation, Formal analysis, Validation, Visualization, Writing – original draft. **Yu Li:** Writing – review & editing, Project administration. **Yong He:** Conceptualization, Project administration. **Zhenjiang Zhou:** Formal analysis, Writing – review & editing. **Lingzhen Ye:** Data curation, Project administration. **Hui Fang:** Data curation, Writing – review & editing. **Yiqi Luo:** Writing – review & editing. **Xuping Feng:** Conceptualization, Supervision, Funding acquisition, Writing - review & editing.

## Declaration of Competing Interest

The authors declare that they have no known competing financial interests or personal relationships that could have appeared to influence the work reported in this paper.

## Acknowledgments

Thanks to the Changxing Agricultural Experiment Station of Zhejiang University and the Yuhang Agricultural Experiment Station of Zhejiang University for providing the experimental base. Thanks to Professor Xianchun Xia and Dr. Jindong Liu (Chinese Academy of Agricultural Sciences) for providing wheat germplasm resources. Thanks to the members of the Digital Phenotyping Research Group of Zhejiang University for their help in data collection. This research was supported by Zhejiang Provincial Key R&D Program of China (Grant No. 2022C02013).

## Appendix A. Supplementary data

Supplementary material

## Data Availability

The dataset for the current study is available in the Zenodo repository at <https://doi.org/10.5281/zenodo.13736773>.

## References

- AI, 01, Young, A., Chen, B., Li, C., Huang, C., Zhang, Ge, Zhang, Guanwei, Li, H., Zhu, J., Chen, J., Chang, J., Yu, K., Liu, P., Liu, Q., Yue, S., Yang, Senbin, Yang, Shiming, Yu, T., Xie, W., Huang, W., Hu, X., Ren, X., Niu, X., Nie, P., Xu, Y., Liu, Y., Wang, Y., Cai, Y., Gu, Z., Liu, Z., Dai, Z., 2024. Yi: Open Foundation Models by 01.AI. <https://doi.org/10.48550/arXiv.2403.04652>
- Anderegg, J., Tschurr, F., Kirchgessner, N., Treier, S., Schmucki, M., Streit, B., Walter, A., 2023. On-farm evaluation of UAV-based aerial imagery for season-long weed monitoring under contrasting management and pedoclimatic conditions in wheat. *Comput. Electron. Agric.* 204. <https://doi.org/10.1016/j.compag.2022.107558>
- Avola, D., Cinque, L., Fagioli, A., Foresti, G.L., Pannone, D., Piciarelli, C., 2021. Automatic estimation of optimal UAV flight parameters for real-time wide areas monitoring. *Multimed. TOOLS Appl.* 80, 25009–25031. <https://doi.org/10.1007/s11042-021-10859-3>
- Badgley, G., Field, C.B., Berry, J.A., 2017. Canopy near-infrared reflectance and terrestrial photosynthesis. *Sci. Adv.* 3. <https://doi.org/10.1126/sciadv.1602244>
- Bai, J., Bai, S., Yang, S., Wang, S., Tan, S., Wang, P., Lin, J., Zhou, C., Zhou, J., 2023. Qwen-VL: A Versatile Vision-Language Model for Understanding, Localization, Text Reading, and Beyond. <https://doi.org/10.48550/arXiv.2308.12966>
- Balaguer, A., Benara, V., Cunha, R.L. de F., Filho, R. de M.E., Hendry, T., Holstein, D., Marsman, J., Mecklenburg, N., Malvar, S., Nunes, L.O., Padilha, R., Sharp, M., Silva, B., Sharma, S.,

- Aski, V., Chandra, R., 2024. RAG vs Fine-tuning: Pipelines, Tradeoffs, and a Case Study on Agriculture. <https://doi.org/10.48550/arXiv.2401.08406>
- Bhat, J.A., Feng, X., Mir, Z.A.A., Raina, A., Siddique, K.H.M., 2023. Recent advances in artificial intelligence, mechanistic models, and speed breeding offer exciting opportunities for precise and accelerated genomics-assisted breeding. *Physiol. Plant.* 175. <https://doi.org/10.1111/ppl.13969>
- Cai, Z., Cao, M., Chen, H., Chen, Kai, Chen, Keyu, Chen, Xin, Chen, Xun, Chen, Zehui, Chen, Zhi, Chu, P., Dong, X., Duan, H., Fan, Q., Fei, Z., Gao, Y., Ge, J., Gu, C., Gu, Y., Gui, T., Guo, A., Guo, Q., He, C., Hu, Y., Huang, T., Jiang, T., Jiao, P., Jin, Z., Lei, Z., Li, Jiaying, Li, Jingwen, Li, L., Li, S., Li, W., Li, Y., Liu, H., Liu, J., Hong, J., Liu, Kaiwen, Liu, Kuikun, Liu, X., Lv, C., Lv, H., Lv, K., Ma, L., Ma, R., Ma, Z., Ning, W., Ouyang, L., Qiu, J., Qu, Y., Shang, F., Shao, Y., Song, D., Song, Z., Sui, Z., Sun, P., Sun, Y., Tang, H., Wang, B., Wang, G., Wang, Jiaqi, Wang, Jiayu, Wang, R., Wang, Y., Wang, Z., Wei, X., Weng, Q., Wu, F., Xiong, Y., Xu, C., Xu, R., Yan, H., Yan, Y., Yang, X., Ye, H., Ying, H., Yu, Jia, Yu, Jing, Zang, Y., Zhang, C., Zhang, L., Zhang, Pan, Zhang, Peng, Zhang, R., Zhang, Shuo, Zhang, Songyang, Zhang, Wenjian, Zhang, Wenwei, Zhang, Xingcheng, Zhang, Xinyue, Zhao, H., Zhao, Q., Zhao, X., Zhou, F., Zhou, Z., Zhuo, J., Zou, Y., Qiu, X., Qiao, Y., Lin, D., 2024. InternLM2 Technical Report. <https://doi.org/10.48550/arXiv.2403.17297>
- Camps-Valls, G., Campos-Taberner, M., Moreno-Martinez, A., Walther, S., Duveiller, G., Cescatti, A., Mahecha, M.D., Munoz-Mari, J., Javier Garcia-Haro, F., Guanter, L., Jung, M., Gamon, J.A., Reichstein, M., Running, S.W., 2021. A unified vegetation index for quantifying the terrestrial biosphere. *Sci. Adv.* 7. <https://doi.org/10.1126/sciadv.abc7447>
- Cao, Z., Yao, X., Liu, H., Liu, B., Cheng, T., Tian, Y., Cao, W., Zhu, Y., 2019. Comparison of the abilities of vegetation indices and photosynthetic parameters to detect heat stress in wheat. *Agric. For. Meteorol.* 265, 121–136. <https://doi.org/10.1016/j.agrformet.2018.11.009>
- Chen, J., Xiao, S., Zhang, P., Luo, K., Lian, D., Liu, Z., 2024. BGE M3-Embedding: Multi-Lingual, Multi-Functionality, Multi-Granularity Text Embeddings Through Self-Knowledge Distillation. <https://doi.org/10.48550/arXiv.2402.03216>
- Chen, Z., Jia, K., Wei, X., Liu, Y., Zhan, Y., Xia, M., Yao, Y., Zhang, X., 2022. Improving leaf area index estimation accuracy of wheat by involving leaf chlorophyll content information. *Comput. Electron. Agric.* 196. <https://doi.org/10.1016/j.compag.2022.106902>
- Chen, Z., Wang, Weiyun, Tian, H., Ye, S., Gao, Z., Cui, E., Tong, W., Hu, K., Luo, J., Ma, Z., Ma, J., Wang, J., Dong, X., Yan, H., Guo, H., He, C., Shi, B., Jin, Z., Xu, C., Wang, B., Wei, X., Li, W., Zhang, W., Zhang, B., Cai, P., Wen, L., Yan, X., Dou, M., Lu, L., Zhu, X., Lu, T., Lin, D., Qiao, Y., Dai, J., Wang, Wenhai, 2024. How Far Are We to GPT-4V? Closing the Gap to Commercial Multimodal Models with Open-Source Suites. <https://doi.org/10.48550/arXiv.2404.16821>
- Cheng, S., Feng, C., Wingen, L.U., Cheng, H., Riche, A.B., Jiang, M., Leverington-Waite, M., Huang, Z., Collier, S., Orford, S., Wang, Xiaoming, Awal, R., Barker, G., O'Hara, T., Lister, C., Siluveru, A., Quiroz-Chavez, J., Ramirez-Gonzalez, R.H., Bryant, R., Berry, S., Bansal, U., Bariana, H.S., Bennett, M.J., Bicego, B., Bilham, L., Brown, J.K.M., Burridge, A., Burt, C., Buurman, M., Castle, M., Chartrain, L., Chen, B., Denbel, W., Elkot, A.F., Fenwick, P., Feuerhelm, D., Foulkes, J., Gaju, O., Gauley, A., Gaurav, K., Hafeez, A.N., Han, R., Horler, R., Hou, J., Iqbal, M.S., Kerton, M., Kondic-Spica, A., Kowalski, A., Lage, J., Li, X., Liu,

- H., Liu, S., Lovegrove, A., Ma, L., Mumford, C., Parmar, S., Philp, C., Playford, D., Przewieslik-Allen, A.M., Sarfraz, Z., Schafer, D., Shewry, P.R., Shi, Y., Slafer, G., Song, Baoxing, Song, Bo, Steele, D., Steuernagel, B., Tailby, P., Tyrrell, S., Waheed, A., Wamalwa, M.N., Wang, Xingwei, Wei, Y., Winfield, M., Wu, S., Wu, Y., Wulff, B.B.H., Xian, W., Xu, Yawen, Xu, Yunfeng, Yuan, Q., Zhang, X., Edwards, K.J., Dixon, L., Nicholson, P., Chayut, N., Hawkesford, M.J., Uauy, C., Sanders, D., Huang, S., Griffiths, S., 2024. Harnessing landrace diversity empowers wheat breeding. *Nature*. <https://doi.org/10.1038/s41586-024-07682-9>
- Cui, S., Chen, W., Gu, W., Yang, L., Shi, X., 2023. SiamC Transformer: Siamese coupling swin transformer Multi-Scale semantic segmentation network for vegetation extraction under shadow conditions. *Comput. Electron. Agric.* 213. <https://doi.org/10.1016/j.compag.2023.108245>
- Das, S., Christopher, J., Apan, A., Choudhury, M.R., Chapman, S., Menzies, N.W., Dang, Y.P., 2021. Evaluation of water status of wheat genotypes to aid prediction of yield on sodic soils using UAV-thermal imaging and machine learning. *Agric. For. Meteorol.* 307. <https://doi.org/10.1016/j.agrformet.2021.108477>
- DeepSeek-AI, Liu, A., Feng, B., Wang, Bin, Wang, Bingxuan, Liu, B., Zhao, C., Dengr, C., Ruan, C., Dai, D., Guo, D., Yang, D., Chen, D., Ji, D., Li, E., Lin, F., Luo, F., Hao, G., Chen, G., Li, G., Zhang, H., Xu, H., Yang, H., Zhang, Haowei, Ding, H., Xin, H., Gao, H., Li, H., Qu, H., Cai, J.L., Liang, J., Guo, J., Ni, J., Li, J., Chen, J., Yuan, J., Qiu, J., Song, J., Dong, K., Gao, K., Guan, K., Wang, L., Zhang, Lecong, Xu, L., Xia, L., Zhao, L., Zhang, Liyue, Li, Meng, Wang, M., Zhang, Mingchuan, Zhang, Minghua, Tang, M., Li, Mingming, Tian, N., Huang, P., Wang, P., Zhang, P., Zhu, Q., Chen, Q., Du, Q., Chen, R.J., Jin, R.L., Ge, R., Pan, R., Xu, R., Chen, R., Li, S.S., Lu, S., Zhou, Shangyan, Chen, S., Wu, S., Ye, S., Ma, S., Wang, S., Zhou, Shuang, Yu, S., Zhou, Shunfeng, Zheng, S., Wang, T., Pei, T., Yuan, T., Sun, T., Xiao, W.L., Zeng, W., An, W., Liu, W., Liang, W., Gao, W., Zhang, W., Li, X.Q., Jin, X., Wang, Xianzu, Bi, X., Liu, Xiaodong, Wang, Xiaohan, Shen, X., Chen, Xiaokang, Chen, Xiaosha, Nie, X., Sun, X., Wang, Xiaoxiang, Liu, Xin, Xie, X., Yu, X., Song, X., Zhou, X., Yang, X., Lu, X., Su, X., Wu, Y., Li, Y.K., Wei, Y.X., Zhu, Y.X., Xu, Y., Huang, Y., Li, Yao, Zhao, Yao, Sun, Y., Li, Yaohui, Wang, Yaohui, Zheng, Y., Zhang, Y., Xiong, Y., Zhao, Yilong, He, Y., Tang, Y., Piao, Y., Dong, Y., Tan, Y., Liu, Yiyuan, Wang, Yongji, Guo, Y., Zhu, Y., Wang, Yuduan, Zou, Y., Zha, Y., Ma, Y., Yan, Y., You, Y., Liu, Yuxuan, Ren, Z.Z., Ren, Z., Sha, Z., Fu, Z., Huang, Z., Zhang, Zhen, Xie, Zhenda, Hao, Z., Shao, Z., Wen, Z., Xu, Z., Zhang, Zhongyu, Li, Zhuoshu, Wang, Z., Gu, Z., Li, Zilin, Xie, Ziwei, 2024. DeepSeek-V2: A Strong, Economical, and Efficient Mixture-of-Experts Language Model. <https://doi.org/10.48550/arXiv.2405.04434>
- Du, R., Chen, J., Xiang, Y., Zhang, Z., Yang, N., Yang, X., Tang, Z., Wang, H., Wang, X., Shi, H., Li, W., 2023. Incremental learning for crop growth parameters estimation and nitrogen diagnosis from hyperspectral data. *Comput. Electron. Agric.* 215. <https://doi.org/10.1016/j.compag.2023.108356>
- Duan, T., Chapman, S.C., Guo, Y., Zheng, B., 2017. Dynamic monitoring of NDVI in wheat agronomy and breeding trials using an unmanned aerial vehicle. *FIELD CROPS Res.* <https://doi.org/10.1016/j.fcr.2017.05.025>
- Fei, S., Hassan, M.A., Xiao, Y., Su, X., Chen, Z., Cheng, Q., Duan, F., Chen, R., Ma, Y., 2023. UAV-

- based multi-sensor data fusion and machine learning algorithm for yield prediction in wheat. *Precis. Agric.* 24, 187–212. <https://doi.org/10.1007/s11119-022-09938-8>
- Feng, A., Zhou, J., Vories, E., Sudduth, K., 2024. Prediction of cotton yield based on soil texture, weather conditions and UAV imagery using deep learning. *Precis. Agric.* 25, 303–326. <https://doi.org/10.1007/s11119-023-10069-x>
- Feng, Z., Guan, H., Yang, T., He, L., Duan, J., Song, L., Wang, C., Feng, W., 2023. Estimating the canopy chlorophyll content of winter wheat under nitrogen deficiency and powdery mildew stress using machine learning. *Comput. Electron. Agric.* 211. <https://doi.org/10.1016/j.compag.2023.107989>
- Fu, C., Chen, P., Shen, Y., Qin, Y., Zhang, M., Lin, X., Yang, J., Zheng, X., Li, K., Sun, X., Wu, Y., Ji, R., 2024. MME: A Comprehensive Evaluation Benchmark for Multimodal Large Language Models. <https://doi.org/10.48550/arXiv.2306.13394>
- Garg, M., Kaur, S., Sharma, A., Kumari, A., Tiwari, V., Sharma, S., Kapoor, P., Sheoran, B., Goyal, A., Krishania, M., 2022. Rising Demand for Healthy Foods-Anthocyanin Biofortified Colored Wheat Is a New Research Trend. *Front. Nutr.* 9. <https://doi.org/10.3389/fnut.2022.878221>
- Giuffre, M., Kresevic, S., Pugliese, N., You, K., Shung, D.L., 2024. Optimizing large language models in digestive disease: strategies and challenges to improve clinical outcomes. *LIVER Int.* <https://doi.org/10.1111/liv.15974>
- GLM, T., Zeng, A., Xu, B., Wang, B., Zhang, C., Yin, D., Zhang, D., Rojas, D., Feng, G., Zhao, H., Lai, H., Yu, H., Wang, H., Sun, Jiadai, Zhang, Jiajie, Cheng, J., Gui, J., Tang, J., Zhang, Jing, Sun, Jingyu, Li, J., Zhao, L., Wu, L., Zhong, L., Liu, M., Huang, M., Zhang, P., Zheng, Q., Lu, R., Duan, S., Zhang, S., Cao, S., Yang, S., Tam, W.L., Zhao, W., Liu, Xiao, Xia, X., Zhang, Xiaohan, Gu, X., Lv, X., Liu, Xinghan, Liu, Xinyi, Yang, X., Song, X., Zhang, Xunkai, An, Y., Xu, Y., Niu, Y., Yang, Y., Li, Y., Bai, Y., Dong, Y., Qi, Z., Wang, Zhaoyu, Yang, Z., Du, Z., Hou, Z., Wang, Zihan, 2024. ChatGLM: A Family of Large Language Models from GLM-130B to GLM-4 All Tools. <https://doi.org/10.48550/arXiv.2406.12793>
- Gu, Y., Wang, Y., Wu, Y., Warner, T., Guo, T., Ai, H., Zheng, H., Cheng, T., Zhu, Y., Cao, W., Yao, X., 2024. Novel 3D photosynthetic traits derived from the fusion of UAV LiDAR point cloud and multispectral imagery in wheat. *REMOTE Sens. Environ.* 311. <https://doi.org/10.1016/j.rse.2024.114244>
- Hu, N., Du, C., Zhang, W., Liu, Y., Zhang, Y., Zhao, Z., Wang, Z., 2022. Did Wheat Breeding Simultaneously Improve Grain Yield and Quality of Wheat Cultivars Releasing over the Past 20 Years in China? *Agron.-BASEL* 12. <https://doi.org/10.3390/agronomy12092109>
- Huang, D., Yan, C., Li, Q., Peng, X., 2024. From Large Language Models to Large Multimodal Models: A Literature Review. *Appl. Sci.-BASEL* 14. <https://doi.org/10.3390/app14125068>
- Huang, X., Ruan, W., Huang, W., Jin, G., Dong, Y., Wu, C., Bensalem, S., Mu, R., Qi, Y., Zhao, X., Cai, K., Zhang, Y., Wu, S., Xu, P., Wu, D., Freitas, A., Mustafa, M.A., 2024. A survey of safety and trustworthiness of large language models through the lens of verification and validation. *Artif. INTELLIGENCE Rev.* <https://doi.org/10.1007/s10462-024-10824-0>
- Huete, A.R., 1988. A soil-adjusted vegetation index (SAVI). *Remote Sens. Environ.* 25, 295–309. [https://doi.org/10.1016/0034-4257\(88\)90106-X](https://doi.org/10.1016/0034-4257(88)90106-X)
- Jiang, Z., Tu, H., Bai, B., Yang, C., Zhao, B., Guo, Z., Liu, Q., Zhao, H., Yang, W., Xiong, L., Zhang, J., 2021. Combining UAV-RGB high-throughput field phenotyping and genome-wide

- association study to reveal genetic variation of rice germplasms in dynamic response to drought stress. *NEW Phytol.* 232, 440–455. <https://doi.org/10.1111/nph.17580>
- Jin, Z., Guo, S., Li, S., Yu, F., Xu, T., 2024. Research on the rice fertiliser decision-making method based on UAV remote sensing data assimilation. *Comput. Electron. Agric.* 216. <https://doi.org/10.1016/j.compag.2023.108508>
- Kaur, B., Sandhu, K.S., Kamal, R., Kaur, K., Singh, J., Roeder, M.S., Muqaddasi, Q.H., 2021. Omics for the Improvement of Abiotic, Biotic, and Agronomic Traits in Major Cereal Crops: Applications, Challenges, and Prospects. *PLANTS-BASEL* 10. <https://doi.org/10.3390/plants10101989>
- Kuska, M.T., Wahabzada, M., Paulus, S., 2024. AI for crop production - Where can large language models (LLMs) provide substantial value? *Comput. Electron. Agric.* 221. <https://doi.org/10.1016/j.compag.2024.108924>
- Li, C., Gan, Z., Yang, Z., Yang, J., Li, L., Wang, L., Gao, J., 2024. Multimodal Foundation Models: From Specialists to General-Purpose Assistants. *Found. TRENDS Comput. Graph. Vis.* 16, 1–214. <https://doi.org/10.1561/06000000110>
- Li, F., Zhang, R., Zhang, H., Zhang, Y., Li, B., Li, W., Ma, Z., Li, C., 2024. LLaVA-NeXT-Interleave: Tackling Multi-image, Video, and 3D in Large Multimodal Models. <https://doi.org/10.48550/arXiv.2407.07895>
- Li, H., Li, X., Zhang, P., Feng, Y., Mi, J., Gao, S., Sheng, L., Ali, M., Yang, Z., Li, L., Fang, W., Wang, W., Qian, Q., Gu, F., Zhou, W., 2024. Smart Breeding Platform: A web-based tool for high-throughput population genetics, phenomics, and genomic selection. *Mol. PLANT* 17, 677–681. <https://doi.org/10.1016/j.molp.2024.03.002>
- Li, J., Xu, M., Xiang, L., Chen, D., Zhuang, W., Yin, X., Li, Z., 2024. Foundation models in smart agriculture: Basics, opportunities, and challenges. *Comput. Electron. Agric.* 222. <https://doi.org/10.1016/j.compag.2024.109032>
- Lin, Z., Guan, S., Zhang, W., Zhang, Huiyan, Li, Y., Zhang, Huaping, 2024. Towards trustworthy LLMs: a review on debiasing and dehallucinating in large language models. *Artif. INTELLIGENCE Rev.* <https://doi.org/10.1007/s10462-024-10896-y>
- Liu, L., Zhan, J., Yan, J., 2024. Engineering the future cereal crops with big biological data: towardan intelligence-driven breeding by design. *J. Genet. Genomics Yi Chuan Xue Bao.* <https://doi.org/10.1016/j.jgg.2024.03.005>
- Liu, Y., Li, Z., Yang, B., Li, C., Yin, X., Liu, C., Jin, L., Bai, X., 2024. On the Hidden Mystery of OCR in Large Multimodal Models. <https://doi.org/10.48550/arXiv.2305.07895>
- Maimaitijiang, M., Sagan, V., Sidike, P., Hartling, S., Esposito, F., Fritschi, F.B., 2020. Soybean yield prediction from UAV using multimodal data fusion and deep learning. *REMOTE Sens. Environ.* <https://doi.org/10.1016/j.rse.2019.111599>
- Min, B., Ross, H., Sulem, E., Ben Veyseh, A.P., Nguyen, T.H., Sainz, O., Agirre, E., Heintz, I., Roth, D., 2024. Recent Advances in Natural Language Processing via Large Pre-trained Language Models: A Survey. *ACM Comput. Surv.* 56. <https://doi.org/10.1145/3605943>
- Ming, Y., Li, Y., 2024. How Does Fine-Tuning Impact Out-of-Distribution Detection for Vision-Language Models? *Int. J. Comput. Vis.* <https://doi.org/10.1007/s11263-023-01895-7>
- National Bureau of Statistics of China, 2022. *China Rural Statistical Yearbook: 2022.* China Statistics Press, Beijing.
- Padhy, A.K., Kaur, P., Singh, S., Kashyap, L., Sharma, A., 2024. Colored wheat and derived products:

- key to global nutritional security. *Crit. Rev. FOOD Sci. Nutr.* 64, 1894–1910. <https://doi.org/10.1080/10408398.2022.2119366>
- Richardson, A.J., Everitt, J.H., 1992. Using spectral vegetation indices to estimate rangeland productivity. *Geocarto Int.* 7, 63–69. <https://doi.org/10.1080/10106049209354353>
- Roth, L., Barendregt, C., Betrix, C.-A., Hund, A., Walter, A., 2022. High-throughput field phenotyping of soybean: Spotting an ideotype. *REMOTE Sens. Environ.* <https://doi.org/10.1016/j.rse.2021.112797>
- Ruan, G., Li, X., Yuan, F., Cammarano, D., Ata-UI-Karim, S., Liu, X., Tian, Y., Zhu, Y., Cao, W., Cao, Q., 2022. Improving wheat yield prediction integrating proximal sensing and weather data with machine learning. *Comput. Electron. Agric.* 195. <https://doi.org/10.1016/j.compag.2022.106852>
- Sansaloni, C., Franco, J., Santos, B., Percival-Alwyn, L., Singh, S., Petroli, C., Campos, J., Dreher, K., Payne, T., Marshall, D., Kilian, B., Milne, I., Raubach, S., Shaw, P., Stephen, G., Carling, J., Saint Pierre, C., Burgueno, J., Crosa, J., Li, H., Guzman, C., Kehel, Z., Amri, A., Kilian, A., Wenzl, P., Uauy, C., Banziger, M., Caccamo, M., Pixley, K., 2020. Diversity analysis of 80,000 wheat accessions reveals consequences and opportunities of selection footprints. *Nat. Commun.* 11. <https://doi.org/10.1038/s41467-020-18404-w>
- Saskatchewan Seed Growers' Association, 2024. *SaskSeed Guides (2024)*.
- Schulman, J., Wolski, F., Dhariwal, P., Radford, A., Klimov, O., 2017. Proximal Policy Optimization Algorithms. <https://doi.org/10.48550/arXiv.1707.06347>
- Senapati, N., Semenov, M.A., Halford, N.G., Hawkesford, M.J., Asseng, S., Cooper, M., Ewert, F., van Ittersum, M.K., Martre, P., Olesen, J.E., Reynolds, M., Roetter, R.P., Webber, H., 2022. Global wheat production could benefit from closing the genetic yield gap. *Nat. FOOD* 3, 532–541. <https://doi.org/10.1038/s43016-022-00540-9>
- Siriwardhana, S., Weerasekera, R., Wen, E., Kaluarachchi, T., Rana, R., Nanayakkara, S., 2023. Improving the Domain Adaptation of Retrieval Augmented Generation (RAG) Models for Open Domain Question Answering. *Trans. Assoc. Comput. Linguist.* [https://doi.org/10.1162/tacl\\_a\\_00530](https://doi.org/10.1162/tacl_a_00530)
- Skobalski, J., Sagan, V., Alifu, H., Al Akkad, O., Lopes, F.A., Grignola, F., 2024. Bridging the gap between crop breeding and GeoAI: Soybean yield prediction from multispectral UAV images with transfer learning. *ISPRS J. Photogramm. REMOTE Sens.* <https://doi.org/10.1016/j.isprsjprs.2024.03.015>
- State Administration for Market Regulation, Standardization Administration of the P.R.C, 2023. *Wheat*.
- The ModelScope Team, 2024. SWIFT: Scalable lightWeight Infrastructure for Fine-Tuning [WWW Document]. URL <https://github.com/modelscope/swift> (accessed 8.2.24).
- Tian, Z., Zhang, Y., Liu, K., Li, Z., Li, M., Zhang, H., Wu, J., 2022. UAV Remote Sensing Prediction Method of Winter Wheat Yield Based on the Fused Features of Crop and Soil. *REMOTE Sens.* 14. <https://doi.org/10.3390/rs14195054>
- Tucker, C.J., 1979. Red and photographic infrared linear combinations for monitoring vegetation. *Remote Sens. Environ.* 8, 127–150. [https://doi.org/10.1016/0034-4257\(79\)90013-0](https://doi.org/10.1016/0034-4257(79)90013-0)
- Wang, X., Chen, G., Qian, G., Gao, P., Wei, X.-Y., Wang, Y., Tian, Y., Gao, W., 2023. Large-scale Multi-modal Pre-trained Models: A Comprehensive Survey. *Mach. Intell. Res.* 20, 447–482. <https://doi.org/10.1007/s11633-022-1410-8>

- Xiong, W., Reynolds, M.P., Crossa, J., Schulthess, U., Sonder, K., Montes, C., Addimando, N., Singh, R.P., Ammar, K., Gerard, B., Payne, T., 2021. Increased ranking change in wheat breeding under climate change. *Nat. PLANTS*. <https://doi.org/10.1038/s41477-021-00988-w>
- Xu, J., Zhu, C., Su, M., Li, S., Chao, H., Chen, M., 2023. CropGF: a comprehensive visual platform for crop gene family mining and analysis. *DATABASE- J. Biol. DATABASES CURATION* 2023. <https://doi.org/10.1093/database/baad051>
- Xu, T., Wang, F., Shi, Z., Xie, L., Yao, X., 2023. Dynamic estimation of rice aboveground biomass based on spectral and spatial information extracted from hyperspectral remote sensing images at different combinations of growth stages. *ISPRS J. Photogramm. REMOTE Sens.* <https://doi.org/10.1016/j.isprsjprs.2023.05.021>
- Xu, Y., Zhang, X., Li, H., Zheng, H., Zhang, J., Olsen, M.S., Varshney, R.K., Prasanna, B.M., Qian, Q., 2022. Smart breeding driven by big data, artificial intelligence, and integrated genomic-enviromic prediction. *Mol. PLANT* 15, 1664–1695. <https://doi.org/10.1016/j.molp.2022.09.001>
- Yang, G., He, Y., Zhou, Z., Huang, L., Li, X., Yu, Z., Yang, Y., Li, Y., Ye, L., Feng, X., 2022. Field Monitoring of Fractional Vegetation Cover Based on UAV Low-altitude Remote Sensing and Machine Learning, in: 2022 10th International Conference on Agro-Geoinformatics (Agro-Geoinformatics). pp. 1–6. <https://doi.org/10.1109/Agro-Geoinformatics55649.2022.9859063>
- Yang, G., Li, X., Liu, P., Yao, X., Zhu, Y., Cao, W., Cheng, T., 2023. Automated in-season mapping of winter wheat in China with training data generation and model transfer. *ISPRS J. Photogramm. REMOTE Sens.* <https://doi.org/10.1016/j.isprsjprs.2023.07.004>
- Yao, E., Blake, V.C., Cooper, L., Wight, C.P., Michel, S., Cagirici, H.B., Lazo, G.R., Birkett, C.L., Waring, D.J., Jannink, J.-L., Holmes, I., Waters, A.J., Eickholt, D.P., Sen, T.Z., 2022. GrainGenes: a data-rich repository for small grains genetics and genomics. *DATABASE- J. Biol. DATABASES CURATION* 2022. <https://doi.org/10.1093/database/baac034>
- Yuan, Y., Hao, J., Ma, Y., Dong, Z., Liang, H., Liu, J., Feng, Z., Zhao, K., Zheng, Y., 2024. Uni-RLHF: Universal Platform and Benchmark Suite for Reinforcement Learning with Diverse Human Feedback. Presented at the The Twelfth International Conference on Learning Representations.
- Yue, X., Ni, Y., Zhang, K., Zheng, T., Liu, R., Zhang, G., Stevens, S., Jiang, D., Ren, W., Sun, Y., Wei, C., Yu, B., Yuan, R., Sun, R., Yin, M., Zheng, B., Yang, Z., Liu, Y., Huang, W., Sun, H., Su, Y., Chen, W., 2024. MMMU: A Massive Multi-discipline Multimodal Understanding and Reasoning Benchmark for Expert AGI. <https://doi.org/10.48550/arXiv.2311.16502>
- Zhang, B., Gu, L., Dai, M., Bao, X., Sun, Q., Zhang, M., Qu, X., Li, Z., Zhen, W., Gu, X., 2024. Estimation of grain filling rate of winter wheat using leaf chlorophyll and LAI extracted from UAV images. *FIELD CROPS Res.* 306. <https://doi.org/10.1016/j.fcr.2023.109198>
- Zhang, G., Yan, H., Zhang, D., Zhang, H., Cheng, T., Hu, G., Shen, S., Xu, H., 2023. Enhancing model performance in detecting lodging areas in wheat fields using UAV RGB Imagery: Considering spatial and temporal variations. *Comput. Electron. Agric.* <https://doi.org/10.1016/j.compag.2023.108297>
- Zhu, J., Yang, G., Feng, X., Li, X., Fang, H., Zhang, J., Bai, X., Tao, M., He, Y., 2022. Detecting

Wheat Heads from UAV Low-Altitude Remote Sensing Images Using Deep Learning Based on Transformer. *REMOTE Sens.* 14. <https://doi.org/10.3390/rs14205141>

Zhu, W., Han, R., Shang, X., Zhou, T., Liang, C., Qin, X., Chen, H., Feng, Z., Zhang, H., Fan, X., Li, W., Li, L., 2024. The CropGPT project: Call for a global, coordinated effort in precision design breeding driven by AI using biological big data. *Mol. PLANT* 17, 215–218. <https://doi.org/10.1016/j.molp.2023.12.015>